monoclonal antibody (2 μg/ml in PBS; 05-636; Upstate Biotechnology Inc., Lake Placid, NY, USA) for 1 hr at room temperature. Next, the cells were rinsed with ice-cold PBS and treated with the secondary antibody, Alexa Flour 488 anti-mouse IgG (1/1,000 diluted in PBS; A11029; Molecular Probe, Junction City, OR, USA), for 1 hr. After the cells had been rinsed with ice-cold PBS, they were soaked in Vectashield mounting solution containing 4',6-diamino-2-phenylindole dihydrochloride (DAPI) (H-1200; Vector Laboratories, Inc., Burlingame, CA, USA) and overlaid with a cover glass. Fluorescent images of the cell nuclei were obtained at a magnification of × 1,000 using a fluorescence microscope (BX-URA2; Olympus Co., Tokyo, Japan) and a cooled CCD camera (VB-7000; Keyence Co., Osaka, Japan). The DAPI-stained nuclei and γH2AX foci appeared blue and green, respectively. Thus, the blue and green areas of each nucleus were measured using an image analyzing system (VH-H1A5; Keyence Co.). The value of the green area divided by the total (blue+green) area was used to represent the relative level of H2AX phosphorylation.

SCE test

The SCE test was performed as described previously (Kato *et al.*, 2012). Briefly, CHO AA8 cells were cultured in RPMI 1640 (Sigma-Aldrich Japan) supplemented with 10% fetal bovine serum (JRH Biosciences) at 37°C in a 5% CO_2 atmosphere. The cells were treated with the nanoparticles for 1 hr as described above and then cultured in medium containing 10% serum and 10 μg/ml 5-bromodeoxyuridine (Sigma-Aldrich Japan) for 26 hr. Colcemid (Nacalai Tesque) was added for the last 2 hr at a final concentration of 60 ng/ml. The cells were then trypsinized and centrifuged, resuspended in 0.075 M KCl, and incubated for 30 min, before being fixed four times in methanol:glacial acetic acid (3:1). The cell solution was dropped onto slides in a HANABI Metaphase Spreader (AD Science Technology, Funabashi, Japan). The slides were then soaked in 50 μg/ml Hoechst #33258 (Sigma-Aldrich, St. Louis, MO, USA), before being covered with 0.01 M sodium phosphate buffer (pH 7.6) and cover glasses and irradiated with black light at 365 nm for 3 hr. Subsequently, the slides were stained with 6% Giemsa stain (Merck KGaA, Darmstadt, Germany) in 0.06 M sodium phosphate buffer (pH 6.4) for 15 min. SCE was scored under a microscope. At least 50 cells were observed in each experiment.

Detection of ROS

CellROX Deep Red Reagent (Life Technologies, Carlsbad, CA, USA) was used to detect ROS according to the manufacturer's instructions. Briefly, CHO AA8 cells (2×10^5 cells/well) were seeded in 6-well plates a day before the experiment. The cells were treated with the nanoparticles for 1 hr, as described in the section "Detection of γH2AX", and then CellROX Deep Red Reagent was added to them at a final concentration of 5 μM, before the cells were incubated with the nanoparticles for further 30 min at 37°C. Then, the cells were washed with PBS and recovered with trypsin treatment. In the experiments involving anti-oxidant exposure (NAC, α-tocopherol, or ascorbic acid; Nacalai Tesque), the cells were cultured with medium containing the indicated concentrations of anti-oxidants for 1 hr before the treatment. Then, the cells were treated with the nanoparticles for 1 hr and cultured further with the nanoparticles and CellROX Deep Red Reagent for 0.5 hr in the presence of the anti-oxidant. The fluorescence intensity produced by the CellROX Deep Red Reagent was determined with flow cytometry (FCM) (Accuri C6 flow cytometer; Becton Dickinson, Franklin Lakes, NJ, USA). At least 10,000 cells per sample were analyzed.

Statistical analysis

The Tukey-Kramer method or Student's t-test was used to compare the difference in means between the treated and control groups using R 2.10.1 or Microsoft Excel 2004 software, respectively. One-way analysis of variance (ANOVA) was carried out using Microsoft Excel 2004 software in order to show the effect of concentration, where appropriate. A p value < 0.05 was considered statistically significant.

RESULTS AND DISCUSSION

Induction of micronucleus formation

The MN-inducing activity of the magnetite nanoparticles was examined using the human lung cancer cell line A549. Six hours' treatment with 200 μg/ml (34 μg/cm²) magnetite inhibited the growth of the A549 cells by 69.2% (data not shown). As shown in Fig. 1, the magnetite nanoparticles increased the number of micronucleated cells in a dose-dependent manner. The background frequency of micronucleated cells was 1.8%, and the frequency rose to 5.2% at a magnetite concentration of 200 μg/ml (34 μg/cm²). The increase in the frequency of micronucleated cells was statistically significant ($p < 0.05$) at all of the magnetite particle concentrations tested. This confirmed that magnetite nanoparticles induce MN formation in A549 cells, as was reported by Konczol *et al.* (2011). Note that they did not observe MN induction after low dose exposure (1 μg/cm²

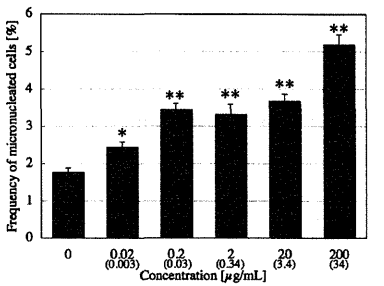

Fig. 1. Micronuclei formation in human A549 cells after 6 hours' treatment with magnetite nanoparticles. Mean ± S.D. values of at least 1,000 cells are shown. In the graph, 0 represents the solvent control (treatment with 0.005% (v/v) Tween 80). Concentrations in μg/cm² are given in parenthesis. There was a significant effect of concentration in one-way ANOVA ($p < 0.01$); $*p < 0.05$, $**p < 0.01$ (versus the solvent control) according to the Tukey-Kramer method.

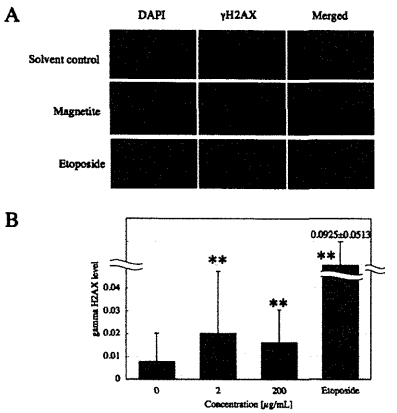

Fig. 2. γH2AX foci induced in A549 cells by 1 hour's treatment with magnetite nanoparticles. A, Magnified images of γH2AX foci in the cells treated with 0.005% (v/v) Tween 80 as a solvent control, 200 μg/ml magnetite nanoparticles, or 100 μg/ml etoposide as a positive control. B, Relative level of γH2AX. Mean ± S.D. values of at least 100 cells are shown. In the graph, 0 represents the solvent control (treatment with 0.005% (v/v) Tween 80). Etoposide (100 μg/ml) was used as a positive control. There was a significant effect of concentration of magnetite nanoparticles in one-way ANOVA ($p < 0.01$); $**p < 0.01$ (versus the solvent control) according to the Tukey-Kramer method.

for 24 hr) (Konczol *et al.*, 2011). We used Tween 80 as a surfactant to prepare the particle suspension. The difference in the dispersion procedure influences agglomeration of the particle, and might affect the toxicity in the low dose range.

In our experiment, the magnetite particles induced MN formation in CHO AA8 cells as well (Fig. 5A). The frequency rose to 5.0% at a magnetite concentration of 200 μg/ml (34 μg/cm²).

Formation of γ-H2AX foci

Since MN formation can be caused by DSB, the frequency of DSB in the cells treated with magnetite particles was evaluated by detecting phosphorylated H2AX (Fig. 2). The treatment of A549 cells with the nanoparticles for 1 hr induced H2AX phosphorylation (Fig. 2A). The relative levels of H2AX phosphorylation in the treated cells were two times higher than the control level (Fig. 2B), and the increase was significant ($p < 0.01$) at magnetite nanoparticle concentrations of 2 μg/ml or higher. In addition to DSB, various other forms of DNA damage can also induce the formation of γH2AX foci since DNA damage induces replication arrest, which causes DSB (Friedberg *et al.*, 2006). Therefore, the observed increase in the number of γH2AX foci indicates that the magnetite nanoparticles induced DSB in a direct or indirect manner in the A549 cells. Using the comet assay, Konczol *et al.* (2011) also detected increased DNA migration in A549 cells that had been treated with magnetite nanoparticles, which was indicative of treatment-induced DNA damage. Our findings are consistent with theirs.

Induction of SCE

DNA damage including DSB is known to induce SCE. Thus, we evaluated the clastogenic activity of magnetite nanoparticles using the SCE test. It is easier to observe chromatids in Chinese hamster cells than in human cells since Chinese hamster cells have fewer chromosomes than humans. As the magnetite particles induced MN formation in the CHO AA8 cells as well (Fig. 5A), we performed the SCE test using CHO AA8 cells (Fig. 3). An SCE frequency of approximately five times the control

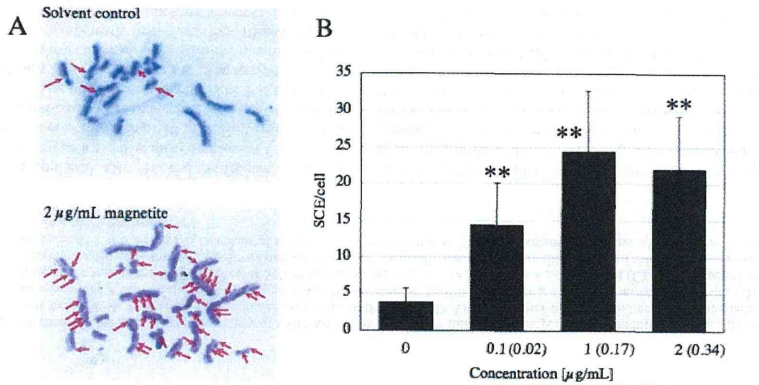

Fig. 3. SCE in CHO AA8 cells following 1 hour's treatment with magnetite nanoparticles. A, Typical images of SCE. The arrows indicate the locations of SCE. B, The number of SCE events per cell. Mean ± S.D. values of at least 50 cells are shown. In the graph, 0 represents the solvent control (treatment with 0.005% (v/v) Tween 80). Concentrations in μg/cm² are given in parenthesis. There was a significant effect of concentration in one-way ANOVA ($p < 0.01$); **$p < 0.01$ (versus the solvent control) according to the Tukey-Kramer method.

level was observed in the cultures treated with 2 μg/ml (0.34 μg/cm²) of the magnetite particles. This increase was significant ($p < 0.01$) at concentrations of 0.1 μg/ml (0.017 μg/cm²) or higher. This is the first report to find that magnetite nanoparticles induce SCE in mammalian cells. The results of the MN and SCE tests indicate that magnetite nanoparticles have clastogenic potency in cultured mammalian cells.

Generation of reactive oxygen species

The generation of ROS in CHO cells that had been treated with magnetite particles was examined using FCM. After the cells had been treated with the particles for 1.5 hr, dose-dependent increases in the numbers of ROS signals were detected (Fig. 4A). Whereas only 9.8% of the cells displayed fluorescent intensity of greater than 10^4 arbitrary unit in the solvent control, treatment with magnetite particle concentrations of 2 μg/ml and 20 μg/ml resulted in 19.8% and 95.5% of the cells displaying fluorescent intensity of greater than 10^4 arbitrary unit, respectively. The number of ROS signals was decreased in the presence of anti-oxidants (Fig. 4B). The addition of NAC, ascorbic acid (vitamin C), or α-tocopherol (vitamin E) decreased the fluorescent intensity of the cells. Ascorbic acid and α-tocopherol reduced ROS to a greater degree than NAC. These results indicate that the magnetite particles induced ROS production in the CHO cells. Increase of ROS signals in A549 cells treated with magnetite particles and decrease of the signals in the presence of NAC were also observed (data not shown). Previous studies have also detected ROS generation in A549 cells treated with magnetite nanoparticles (Konczol *et al.*, 2011).

The mechanism of ROS production by magnetite is still unclear. Particles can damage mitochondria, therefore, interaction between magnetite and mitochondria could be responsible to the ROS generation (Konczol *et al.*, 2011). Membrane-bound NADPH oxidases could enhance production of ROS as well. Uptake of particles via phagocytosis can lead to an activation of the membrane-bound NADPH oxidase, which catalyzes the conversion of oxygen to superoxide radicals (Konczol *et al.*, 2011; Nabeshi *et al.*, 2011).

Note that although treatment with the particle concentrations of 20 μg/ml induced much higher ROS signals than that with 2 μg/ml, the genotoxic effects were similar

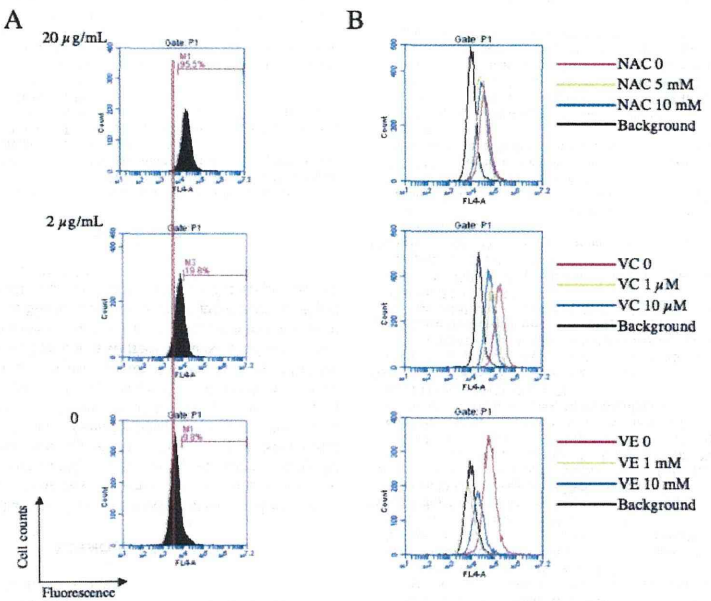

Fig. 4. Flow cytometric analysis of ROS production in CHO AA8 cells after treatment with magnetite nanoparticles. A, Distribution of ROS signals (fluorescence produced by CellROX Deep Red) in the cells treated with the indicated concentrations of magnetite for 1.5 hr. The vertical red line indicates the maximum distribution of fluorescent signals in the solvent control cells. The percentage of cells that displayed fluorescent intensity of greater than 10^4 arbitrary unit is shown in each graph. B, Distribution of ROS signals in the cells treated with 2 μg/ml magnetite nanoparticles in the presence of various anti-oxidants. NAC, VC, and VE represent *N*-acetylcysteine, ascorbic acid, and α-tocopherol, respectively. Background represents the distributions of cellular fluorescent intensity in the cells treated with anti-oxidants (10 mM NAC or VE, or 10 μM VC) in the absence of magnetite nanoparticles.

between these two doses (Figs. 4 and 5A). Cellar defense mechanism against oxidative stress might affect the genotoxicities.

Reduction of micronucleus formation by anti-oxidants

We investigated the relationship between ROS induction and the clastogenicity of the magnetite particles in mammalian cells. As described above, the magnetite treatment induced MN formation in CHO AA8 cells (Fig. 5A). In the presence of the anti-oxidant NAC, the frequency of micronucleated cells among the cells treated with magnetite nanoparticles was decreased in an NAC-dose dependent manner (Fig. 5B). Among the cells treated with 20 μg/ml (3.4 μg/cm²) magnetite particles, treatment with 5 mM and 10 mM NAC resulted in micronucleated cell frequencies of 72% and 54% of those observed in the absence of NAC, respectively. Konczol *et al.* (2011) also reported decreased MN formation in the presence of NAC, therefore, our data are consistent with theirs. Another anti-oxi-

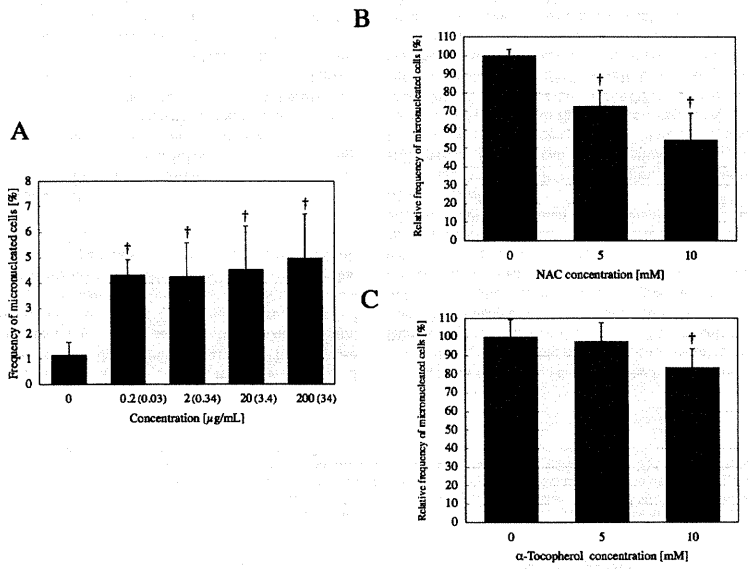

Fig. 5. Decrease in the micronuclei frequency of CHO AA8 cells induced by magnetite nanoparticle treatment in the presence of anti-oxidants. A, Frequency of micronucleated cells among the CHO AA8 cells after 6 hours' treatment with magnetite nanoparticles. Concentrations in μg/cm² are given in parenthesis. †$p < 0.05$ (versus the solvent control) according to the Student's t-test. B and C, Frequency of MN induction in the presence of NAC (B) or α-tocopherol (C). The frequency of micronucleated cells among the cells treated with 20 μg/ml magnetite nanoparticles in the absence of the anti-oxidants was regarded as 100%. Mean ± S.D. values of at least 1,000 cells are shown; †$p < 0.05$ (versus the absence of anti-oxidants) according to the Student's t-test.

dant, α-tocopherol, also reduced the frequency of MN, and it produced a significant reduction in the MN frequency at a concentration of 10 mM. However, the ability of the anti-oxidants to reduce the frequency of MN was not concordant with their effects on ROS. For example, in the MN test NAC reduced the MN frequency to a greater degree than α-tocopherol, whereas α-tocopherol eliminated ROS more efficiently than NAC (Fig. 4B and Figs. 5B, C). The reason for this is unclear; however, ROS might not be the sole cause of the genotoxicity/clastogenicity of magnetite nanoparticles.

In conclusion, we found that manufactured magnetite nanoparticles displayed genotoxicity in *in vitro* assay systems. Our data indicate that magnetite nanoparticles induce ROS production in mammalian cells, leading to the induction of DNA strand breaks directly or indirectly through oxidative DNA damage, followed by clastogenic events including MN formation and SCE. Our observations in A549 cells are consistent with the previous study (Konczol *et al.*, 2011). On the other hand, we observed ROS and MN inductions in CHO cells although Guichard *et al.* (2012) reported that the particles did not increase the ROS or MN formation in Syrian hamster embryo cells. This inconsistency indicates that difference

in cell types and species (genus) would influence the biological effect induced by magnetite nanoparticles. The concentrations of the particles tested in the present study are extremely high compared with the levels encountered by humans in the workplace. Therefore, we cannot conclude magnetite nanoparticles are imminent risk factors on human health. However, the observed *in vitro* genotoxicity of magnetite nanoparticles is a concern because of the large number of individuals that are exposed to such particles. Note that A549 cells have a mutation in keap1 gene, which leads to the constitutive activation of NRF2 that affords the cells with resistance to oxidative stress (Singh *et al.*, 2006; Homma *et al.*, 2009). This nature of the cells may affect the genotoxicity, therefore, genotoxicity assays using A549 cells might underestimate the risk of magnetite nanoparticles. Therefore, further studies on the genotoxicity mechanisms of magnetite particles and the concentrations at which they become hazardous to human health are required.

ACKNOWLEDGEMENTS

We thank Ms. M Fujii for excellent technical assistance. We also thank Ms. M Taniguchi for her assistance to the statistical analyses. This study was supported by the Japanese Ministry of Education, Science, Sports and Culture (Grants-in-aid for Scientific Research for Young Scientists (23710081 to M.K. and 23710084 to K.I.) and for Scientific Research (B) (24310047 to T.Y.)). This study was also supported by the Japanese Ministry of Health, Labor and Welfare (Grants-in-aid for Cancer Research (M.K. and Y.T.) and for Research on the Risk of Chemical Substances (Y.T.)), and a grant from the Japan Chemical Industry Association (JCIA) Long-range Research Initiative (LRI) (Y.T.).

REFERENCES

Ankamwar, B., Lai, T.C., Huang, J.H., Liu, R.S., Hsiao, M., Chen, C.H. and Hwu, Y.K. (2010): Biocompatibility of Fe_3O_4 nanoparticles evaluated by *in vitro* cytotoxicity assays using normal, glia and breast cancer cells. Nanotechnology, **21**, 75102.

Bosi, S., Da Ros, T., Spalluto, G. and Prato, M. (2003): Fullerene derivatives: an attractive tool for biological applications. Eur. J. Med. Chem., **38**, 913-923.

Donaldson, K., Tran, L., Jimenez, L.A., Duffin, R., Newby, D. E., Mills, N., MacNee, W. and Stone, V. (2005): Combustion-derived nanoparticles: a review of their toxicology following inhalation exposure. Part. Fibre Toxicol., **2**, 10.

Elmore, A.R. (2003): Cosmetic Ingredient Review Expert Panel: Final report on the safety assessment of aluminum silicate, calcium silicate, magnesium aluminum silicate, magnesium silicate, magnesium trisilicate, sodium magnesium silicate, zirconium silicate, attapulgite, bentonite, Fuller's earth, hectorite, kaolin, lithium magnesium silicate, lithium magnesium sodium silicate, montmorillonite, pyrophyllite, and zeolite. Int. J. Toxicol., **22 Suppl. 1**, 37-102.

Figuerola, A., Di, C.R., Manna, L. and Pellegrino, T. (2010): From iron oxide nanoparticles towards advanced iron-based inorganic materials designed for biomedical applications. Pharmacol. Res., **62**, 126-143.

Friedberg, E.C., Walker, G.C., Siede, W., Wood, R.D., Schultz, R.A. and Ellenberger, T. (2006): DNA repair and Mutagenesis, ASM press, Washington, D.C., USA.

Guichard, Y., Schmit, J., Darne, C., Gaté, L., Goutet, M., Rousset, D., Rastoix, O., Wrobel, R., Witschger, O., Martin, A., Fierro, V. and Binet, S. (2012): Cytotoxicity and genotoxicity of nanosized and microsized titanium dioxide and iron oxide particles in Syrian hamster embryo cells. Ann. Occup. Hyg., **56**, 631-644.

Hoet, P., Bruske-Hohlfeld, I. and Salata, O. (2006): Possible health impact of nanomaterials. In Nanomaterials - Toxicity, health and environmental issues (Kumar C., ed.), pp.53-80, WILEY-VGH Verlag GmbH & Co. KGaA, Weinheim.

Homma, S., Ishii, Y., Morishima, Y., Yamadori, T., Matsuno, Y., Haraguchi, N., Kikuchi, N., Satoh, H., Sakamoto, T., Hizawa, N., Itoh, K. and Yamamoto, M. (2009): Nrf2 enhances cell proliferation and resistance to anticancer drugs in human lung cancer. Clin. Cancer Res., **15**, 3423-3432.

Hussain, S.M., Hess, K.L., Gearhart, J.M., Geiss, K.T. and Schlager, J.J. (2005): *In vitro* toxicity of nanoparticles in BRL 3A rat liver cells. Toxicol. In Vitro, **19**, 975-983.

IARC (1996): Carbon Black and Some Nitro Compounds. In IARC Monogr. Eval. Carcinog. Risks Hum., **65**, 149-262.

Kato, T., Totsuka, Y., Ishino, K., Matsumoto, Y., Tada, Y., Nakae, D., Goto, S., Masuda, S., Ogo, S., Kawanishi, M., Yagi, T., Matsuda, T., Watanabe, M. and Wakabayashi, K. (2012): Genotoxicity of multi-walled carbon nanotubes in both *in vitro* and *in vivo* assay systems. Nanotoxicology. (in press). doi: 10.3109/17435390.2012.674571.

Konczol, M., Ebeling, S., Goldenberg, E., Treude, F., Gminski, R., Giere, R., Grobety, B., Rothen-Rutishauser, B., Merfort, I. and Mersch-Sundermann, V. (2011): Cytotoxicity and genotoxicity of size-fractionated iron oxide (magnetite) in A549 human lung epithelial cells: role of ROS, JNK, and NF-κB. Chem. Res. Toxicol., **24**, 1460-1475.

Lewinski, N., Colvin, V. and Drezek, R. (2008): Cytotoxicity of nanoparticles. Small, **4**, 26-49.

Mazzola, L. (2003): Commercializing nanotechnology. Nat. Biotechnol., **21**, 1137-1143.

Nabeshi, H., Yoshikawa, T., Matsuyama, K., Nakazato, Y., Tochigi, S., Kondoh, S., Hirai, T., Akase, T., Nagano, K., Abe, Y., Yoshioka, Y., Kamada, H., Itoh, N., Tsunoda, S. and Tsutsumi, Y. (2011): Amorphous nanosilica induce endocytosis-dependent ROS generation and DNA damage in human keratinocytes. Part. Fibre Toxicol., **8**, 1.

Oberdorster, G., Oberdorster, E. and Oberdorster, J. (2005): Nanotoxicology: An emerging discipline evolving from studies of ultrafine particles. Environ. Health Perspect., **113**, 823-839.

Park, E.J., Kim, H., Kim, Y., Yi, J., Choi, K. and Park, K. (2010): Inflammatory responses may be induced by a single intratracheal instillation of iron nanoparticles in mice. Toxicology, **275**, 65-71.

Paull, R., Wolfe, J., Hebert, P. and Sinkula, M. (2003): Investing in nanotechnology. Nat. Biotechnol., **21**, 1144-1147.

Peters, A., Wichmann, H.E., Tuch, T., Heinrich, J. and Heyder, J. (1997): Respiratory effects are associated with the number of

ultrafine particles. Am. J. Respir. Crit. Care Med., **155**, 1376-1383.
Pickard, M.R. and Chari, D.M. (2010): Robust uptake of magnetic nanoparticles (MNPs) by central nervous system (CNS) microglia: Implications for particle uptake in mixed neural cell populations. Int. J. Mol. Sci., **11**, 967-981.
Schulz, H., Harder, V., Ibald-Mulli, A., Khandoga, A., Koenig, W., Krombach, F., Radykewicz, R., Stampfl, A., Thorand, B. and Peters, A. (2005): Cardiovascular effects of fine and ultrafine particles. J. Aerosol. Med., **18**, 1-22.
Shimohara, C. Sawai, T. and Yagi, T. (2008): Polyaromatic hydrocarbons cause histone H2AX phosphorylation in the S-phase of the Cell Cycle. Genes Env., **30**, 92-99.
Singh, A., Misra, V., Thimmulappa, R.K., Lee, H., Ames, S., Hoque, M.O., Herman, J.G., Baylin, S.B., Sidransky, D., Gabrielson, E., Brock, M.V. and Biswal, S. (2006): Dysfunctional KEAP1-NRF2 interaction in non-small-cell lung cancer. PLoS Med., **3**, 1865-1876.
Totsuka, Y., Higuchi, T., Imai, T., Nishikawa, A., Nohmi, T., Kato, T., Masuda, S., Kinae, N., Hiyoshi, K., Ogo, S., Kawanishi, M., Yagi, T., Ichinose, T., Fukumori, N., Watanabe, M., Sugimura, T. and Wakabayashi, K. (2009): Genotoxicity of nano/microparticles in *in vitro* micronuclei, *in vivo* comet and mutation assay systems. Part. Fibre Toxicol., **6**, 23.
Upadhyay, D., Panduri, V., Ghio, A. and Kamp, D.W. (2003): Particulate matter induces alveolar epithelial cell DNA damage and apoptosis: Role of free radicals and the mitochondria. Am. J. Respir. Cell Mol. Biol., **29**, 180-187.

YAKUGAKU ZASSHI **131**(2) 195—201 (2011) © 2011 The Pharmaceutical Society of Japan

—**Review**—

ナノマテリアルの慢性影響研究の重要性

広瀬明彦,[*,a] 高木篤也,[a] 西村哲治,[a] 津田洋幸,[b] 坂本義光,[c]
小縣昭夫,[c] 中江　大,[c] 樋野興夫,[d] 菅野　純[a]

Importance of Researches on Chronic Effects by Manufactured Nanomaterials

Akihiko HIROSE,[*,a] Atsuya TAKAGI,[a] Tetsuji NISHIMURA,[a]
Hiroyuki TSUDA,[b] Yoshimitsu SAKAMOTO,[c] Akio OGATA,[c]
Dai NAKAE,[c] Okio HINO,[d] and Jun KANNO[a]

[a]Division of Risk Assessment, National Institute of Health Sciences, Kamiyoga 1–18–1, Setagaya-ku, Tokyo 158–8501, Japan, [b]Nagoya City of University, 1 Kawasumi Mizuho-cho, Mizuho-ku, Nagoya 467–8601, Japan, [c]Tokyo Metropolitan Institute of Public Health, 3–24–1 Hyakunin-cho, Shinjyuku-ku, Tokyo 169–0073, Japan, and [d]Juntendo University School of Medicine, 2–1–1 Hongo, Bunkyo-ku, Tokyo 113–8421, Japan

(Received September 3, 2010)

Manufactured nanomaterials are the most important substances for the nanotechnology. The nanomaterials possess different physico-chemical properties from bulk materials. The new properties may lead to biologically beneficial effects and/or adverse effects. However, there are no standardized evaluation methods at present. Some domestic research projects and international OECD programs are ongoing, in order to share the health impact information of nanomaterails or to standardize the evaluation methods. From 2005, our institutes have been conducting the research on the establishment of health risk assessment methodology of manufactured nanomaterials. In the course of the research project, we revealed that the nanomaterials were competent to cause chronic effects, by analyzing the intraperitoneal administration studies and carcinogenic promotion studies. These studies suggested that even aggregated nanomaterials were crumbled into nano-sized particles inside the body during the long-term, and the particles were transferred to other organs. Also investigations of the toxicokinetic properties of nanomaterials after exposure are important to predict the chronically targeted tissues. The long lasting particles/fibers in the particular tissues may cause chronic adverse effects. Therefore, focusing on the toxicological characterization of chronic effects was considered to be most appropriate approach for establishing the risk assessment methods of nanomaterials.

Key words——chronic toxicity; multi-wall carbon nanotube (MWCNT); fullerene

1. はじめに

近年，ナノテクノロジーの中心的な役割を担う物質としての産業用ナノマテリアルは，急速にその種類や生産量が増加しつつあるところであるが，新たに期待されているナノマテリアルの物理化学特性については，有効的な生理活性等に使用され得る特性を持つ反面，ヒト健康影響に対する懸念についても検証されるべきであると考えられている．つまり，ナノマテリアルを用いた技術や製品を社会的に受容するためには，安全性の検証を行うことが不可欠であると思われる．しかし，従来の一般的な化学物質とは異なる物理化学的特性は，その毒性評価においても従来とは異なる考え方を取り入れることも必要とされている．それゆえ，ナノマテリアルの特性を考慮した有害性評価手法の開発が急務となっている．また，国際的な枠組みにおいても，ナノマテリアルの安全性確認は，重要な問題として認識されており，OECD や ISO 等を中心として評価手法の国際的標準化に向けた取り組みが進行しているところでもある．本稿では，ナノマテリアルの安全性評価

[a]国立医薬品食品衛生研究所（〒158–8501 東京都世田谷区上用賀 1–18–1），[b]名古屋市立大学（〒467–8601 名古屋市瑞穂区瑞穂町字川澄 1），[c]東京都健康安全研究センター（〒169–0073 東京都新宿区百人町 3–24–1），[d]順天堂大学医学部（〒113–8421 東京都文京区本郷 2–1–1）
*e-mail: hirose@nihs.go.jp

本総説は，日本薬学会第 130 年会シンポジウム S18 で発表したものを中心に記述したものである．

の確立に向けたこれらの取り組みに貢献してきたわれわれの研究成果の一部と，それらの研究結果から帰納的に導き出された慢性影響評価研究の重要性について論ずる．

2. ナノマテリアルのリスク評価法の確立における課題

一般的に，化学物質の健康影響評価（リスクアセスメント）の基本的なフレームは，有害性評価と曝露評価，及び各々の評価内容を比較・統合化する過程のリスク判定のステップから成り立っている．この基本的なフレーム自体は，ナノマテリアルの健康影響評価に適用できるものであると考えられる．[1-5] しかし，ナノマテリアルに特徴的な新たな物理化学的性質，特にサイズが生体内高分子と近いことや，高い表面活性のために凝集し易い性質を考慮すると，よりサイズの大きい通常のバルク化合物や完全に溶解した単一分子化合物とは，生体内挙動が異なることが予想され，同じ化学組成の化合物であってもその毒性発現部位や発現様式は異なることが予想される．つまり，体内動態［吸収 absorption，分布 distribution，代謝 metabolism，排泄 excretion (ADME)］情報は，一般の化学物質より重要な意味を持つと考えられる．

そこで，生体内での挙動を把握するためには，生体試料中で検出，同定・定量できる方法を確立しなくてはならない．一般にナノマテリアルの開発段階において，その性質を把握するための物理化学的測定法も同時に開発されているはずであるが，それらの手法は生体試料中に存在するナノマテリアルにそのまま適用できないことも多い．さらに，機器分析法による生体試料中での検出や定量が可能になったとしても，生体内で実際にナノの状態で存在しているのか，あるいは再凝集などはしていないかなど，標的組織における最終的な生体内反応に影響を及ぼすと考えられる実際のナノマテリアルの存在状態を把握するためには，最終的には，組織標本の電子顕微鏡などによる確認が必要となる．

一方，体内動態に影響を与える因子として，投与法を検討する必要もある．単独では凝集し易いナノマテリアルをそのまま曝露するということは，物理的に巨大となった粒子は体への吸収性が低く，ナノマテリアル自体の体内動態や懸念される有害性を検出することが困難になると考えられるためである．そのために曝露実験時におけるナノマテリアルの分散手法の開発が必要となる．職業曝露などの比較的大量のナノマテリアル曝露の安全性を評価するという観点からは，凝集したままの曝露にも意義があるかもしれないが，製品中への混入や環境中への排出を経由した，分散された曝露も想定されることは考慮すべきであると考えられる．

Figure 1 は，凝集したナノマテリアルが，生体に取り込まれた場合に想定される体内動態を模式図化したものである．ナノマテリアルの使用用途にも依存するが，製品中のナノマテリアルはポリマー等の他の高分子化合物等と混合された状態，あるいはナノマテリアルだけが単独で製品から解離していく状態を考慮しても，この凝集性のために，大きな粒子として曝露する可能性が高いものと想定される．急性的には，このサイズの大きくなった物質は生体に取り込まれることはほとんどなく，局所的な刺激を起こすような変化を除いては，生体内で有害性が惹起される可能性は低いものと考えられる．しかし，仮に凝集したナノマテリアルが長期間に渡って，吸収部位である肺胞や消化管，損傷皮膚などの局所に滞留したり，慢性的に曝露したりするケースを想定すると，時間経過とともに小さくなった凝集体の粒子を除去するために，マクロファージなどの食細胞による取り込みや，表面活性の高いナノマテリアル分子と生体成分との結合作用による侵食作用により，生体に少しずつ取り込まれることが想定される．もしも生体内に取り込まれたナノマテリアルと生体内成分との結合性が高い場合には，容易に生体外に排出されることはなく，特定の組織等へ蓄積し易くなり，慢性影響の可能性を検討する必要が出てくると想定できる．

3. 国立医薬品食品衛生研究所における取り組みの成果の概要

以上のナノマテリアル固有の検討課題を考慮して，われわれは 2005 年より厚生労働科学研究の化学物質リスク研究事業の枠組みの中で，ナノマテリアルの健康影響評価手法の開発に係わる研究を推し進めてきたところである．われわれは，これらの検討課題を解決するために，Fig. 2 に示すように 4 つの項目を中心に研究を行ってきた．これらの項目の中で，*in vivo* 研究については，比較的研究初期の段階から中心的に取り組んできた．その中で，繊維

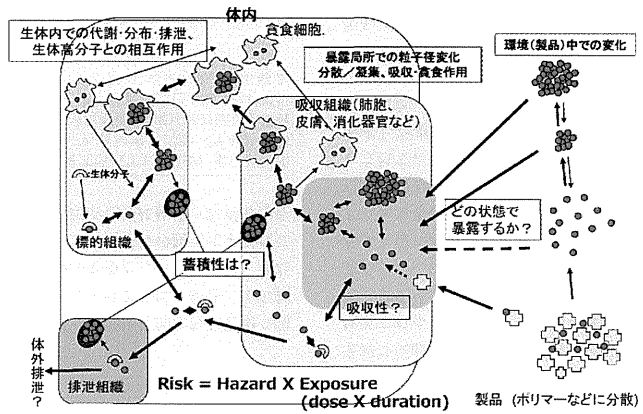

Fig. 1. The Estimated ADME Schema of Nanomaterials

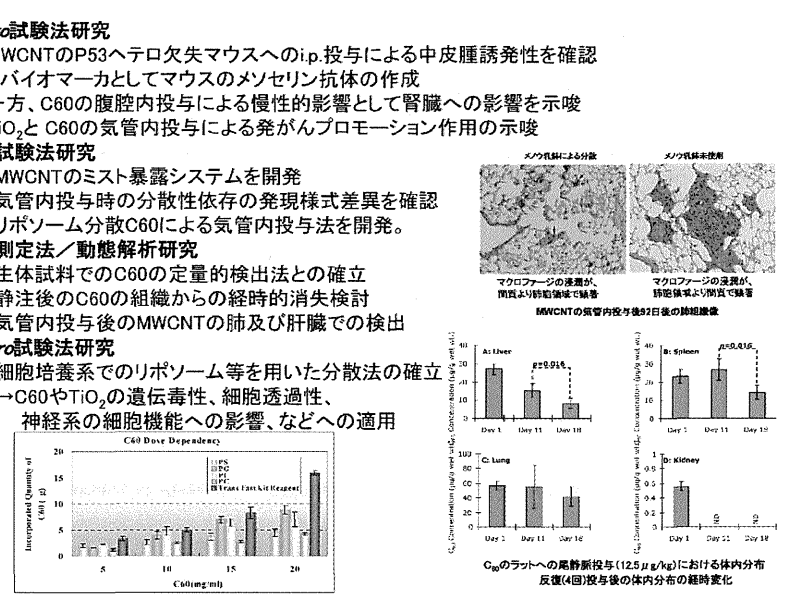

Fig. 2. The Overall Results of NIHS Projects for Nanomaterial Safety

長の長いタイプの多層型カーボンナノチューブ（MWCNT）が，中皮腫を誘発する可能性を持つことを確認した.[6] 上記の体内動態の重要性を考慮した概念からは，吸収性や体内分布について検証したのちに，慢性影響の可能性を検討することが論理的であるが，研究開始当時から，大量生産可能であった，酸化チタン（TiO_2）やフラーレン（C60），MWCNTについては，*in vivo* の慢性影響を先行して検討しておくべきであると判断した．特にその形状がアスベストに似ていたMWCNTについては，吸入曝露による有害影響が懸念されたが，MWCNTについての吸入曝露法が確立していない段階では，アスベストでも検証に使用されていた腹腔内投与による中皮腫誘発試験を行うこととした．

われわれの最初の実験は，アスベストで中皮腫の誘発時期が早くなることが知られているp53ヘテロノックアウトマウスへの腹腔内へ3 mg/mouseという高用量を投与することによって確認されたものであり，動物種の特異性や投与量の多さについて異論も指摘された．しかしその後の研究で，野生型の動物種であるF344ラットに対しても，同じMWCNTが中皮腫の誘発作用を持つことが確認された[7]ほか，投与量を1000分の1にまで少なくした実験においても中皮腫の起きることが示されている（投稿中）．

酸化チタンについては，雌ラットへの吸入曝露により発がん性のあることが示されているが，ナノサイズ化による発がん性の検証のために，気管内投与による肺がんのプロモーション作用の検討を行った．その結果，酸化チタンは，肺腺腫や乳腺腫に対してプロモーション作用を示し，その作用は，マクロファージから放出される炎症性因子であるMIP1αを介したものであることが示唆された.[8] 現在C60やMWCNTを用いたプロモーション作用の検討が進行中である．

一方，曝露手法の開発においては，ミスト法や粉体法によるMWCNTの吸入曝露システムの開発研究を進めているが，より簡易な手法として気管内投与のための適切な分散法の検討を行った．その結果，分散法の違いが肺の有害性発現様式に違いを引き起こすことを確認した.[9]

体内動態解析のために，生体試料中のC60やTiO_2の分析手法の開発や改良を行い，経口投与や気管内投与による体内吸収性について検討を行っている．現在のところ投与部位である消化管や肺以外で有意な検出量を確認できておらず，感度の向上に向けた研究を進めている．しかし，体内への吸収を前提にした解析として，C60の静脈内投与による解析を行ったところ，肝臓や脾臓，肺などへの分布を確認したが，腎臓への分布は極めて低いことが示された（投稿中）．その他，遺伝毒性や標的臓器などの毒性をスクリーニングするための *in vitro* 試験における培地等への分散法も検討対象としており，リポソームを用いたC60の分散法を確立した．

4. 慢性影響研究の重要性

ナノマテリアルの生体影響に関する情報はここ数年の活発な研究状況を反映して多くなりつつあるが，慢性影響に関する報告は依然その数が少ない状況である．一般の化学物質の有害性評価の常套手段として，変異原性試験や短期試験から情報を収集していくことは，必要なステップであり，OECDにおけるナノマテリアル作業グループの活動におけるスポンサーシッププログラムにおいても，加盟各国からの毒性試験情報として，短期試験を中心に収集されてきている．われわれの研究グループにおいても，これらの枠組みに対して，短期的な試験情報を中心に提供し始めている段階である．しかしMWCNTに関しては，研究初期から，短期毒性より長期毒性の方が懸念の強いことが，物性等の情報から推測されたところでもあり，その推定に基づいて，腹腔内投与の研究を最初にスタートさせた．腹腔内投与は，リスク評価の観点からは，曝露経路（吸入曝露）に伴う定量的な評価に問題のあるところであるが，最近の注目すべき研究として，分散剤で分散させたMWCNT（最高80 μgまで）をマウスに吸引させた研究や，MWCNT: 30 mg/m³をマウスに単回吸入曝露した研究において，曝露後7–8週間目にMWCNTが胸膜に到達していたことが報告されている.[10,11] これらの研究結果は高用量の曝露による短期間の結果ではあるが，呼吸器を経由した曝露においてもMWCNTは胸膜（中皮）まで到達することを示唆しており，われわれの腹腔内投与による結果と合わせると，リスク評価の上でも重要な知見であると考えられる．

これらの腹腔内投与による中皮腫誘発能は，繊維状粒子による催腫瘍性のみを検出する系であり，短いタイプやその他様々な形状のMWCNTにおける慢性毒性は別途検証する必要性がある．実際，われわれの行った腹腔内投与試験では，小さいサイズのナノチューブ繊維を含んだ細胞が腹膜の病変部のみならず，肝類洞内，又は肝葉間や腸間膜リンパ節の中にも認められ，体内に再分布することが示唆された（Fig. 3）.[6] さらに，SWCNTをマウスへ咽頭吸引させた実験では，一過性の急性症状の後に，炎症性細胞浸潤を伴わない間質の繊維化が認められている.[12] また，ApoEノックアウトマウスを用いた実験では，タンパクカルボニル化活性の変化を伴うミトコンドリアDNA障害と，アテローム性動脈硬化症の進行を増強することが示された.[13] MWCNTに関しても，マウスにMWCNT（200–400 μg）を気管内滴下した実験では，一過性の肺の炎症反応に加え，投与量に依存した血小板の活性化と凝固作用の活性化の促進が示唆されている.[14] また，MWCNTやSWCNTの気管内投与や経鼻投与により，アレルギー反応の増強反応が報告されている.[15–17] これらの結果が，カーボンナノチューブが直接体内循環に侵入した結果であるか，免疫細胞との接触を介した反応であるかを区別することは難しいが，曝露局所に留まらない全身作用の可能性を示している．われわれの酸化チタンの気管内投与による発がんプロモーション作用が，炎症因子により介在されたことは，これらの知見と同様の作用様式を示すものととらえることもできる．

以上の知見は，短期の試験だけでは検証することは困難であり，ナノマテリアルの有害性を確認するためには，長期の体内動態予測や慢性影響に関する研究が，重要なステップであることを示している．Figure 4にスクリーニング試験や確定試験を開発するための手順についてまとめた．通常の化学物質については，その長い歴史の中で明らかとなった有害性に対して，それぞれの毒性発現様式に応じてスクリーニング試験が開発され，現在まで運用されてきている．特に変異原性試験は発がん性を予測する試験としての重要な役割を担っている．しかし，現時点ではナノマテリアルによる有害性影響が，これまでの研究経験の中で明らかとなった影響だけに留まるのかについては，まだ誰も判定できない状況である．これまでの一般化学物質に対応する有害性とスクリーニング試験を活用して進めていくと同時に，未知の影響を見極める最初のステップとして，少な

腹腔内投与によるナノサイズ粒子の体内再分布

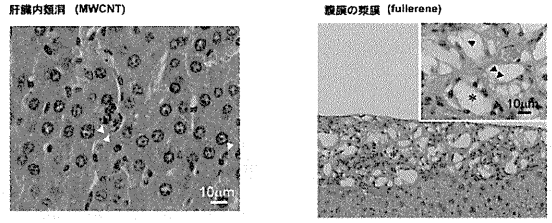

A. Takagi et al., J. Toxicol. Scie., **33**,105-116. (2008)

SWCNTやMWCNTによる全身性影響の示唆

- アテローム性動脈硬化症の進行の増強の可能性（ApoE⁻/⁻マウス）
  Z. Li *et al.*, *Environmental health perspectives*. **115**, 377-382 (2007)
- 血小板の活性化と凝固作用の活性化（MWCNT気管内滴下）
  A. Nemmar *et al.*, *J. Thrombosis, Haemostasis* **5**: 1217-1226 (2007)
- アレルギー反応の増強（MWCNT・SWCNT、気管内・経鼻投与）
  E.J. Park *et al.*, *Toxicology*. **259**, 113-21 (2009)
  U.C. Nygaard *et al.*, *Toxicol Sci*. **109**, 113-23 (2009)
  K. Inoue *et al.*, *Toxicol Appl Pharmacol*. **237**, 306-16 (2009)

Fig. 3. The Suggestive Evidences for Systemic Toxicites by Nanomaterials

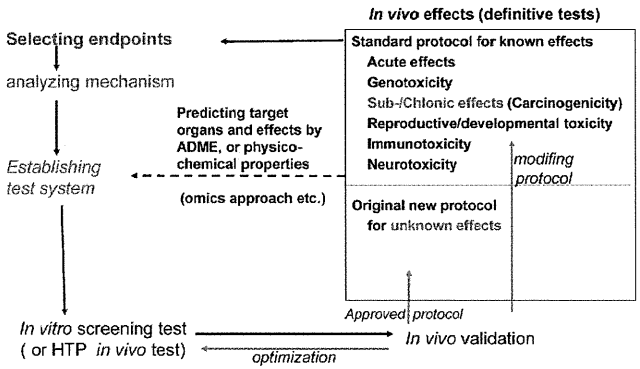

Fig. 4. The Schematic Development of Screening Tests and Definitive Tests

くとも代表的なナノマテリアルによる *in vivo* の慢性影響研究や，その影響を推定するためのナノマテリアルと生体成分との分子レベルでの相互作用や体内残留性様式の解析を進めていくべきであると考えられる．

謝辞　本稿で解説した研究成果の一部は，厚生労働科学研究費補助金（化学物質リスク研究事業）H17-化学-012，H18-化学-一般-007 及び H21-化学-一般-008 の助成によって行われたものです．

REFERENCES

1) Scientific Committee on Emerging and Newly Identified Health Risks, SCENIHR: ⟨http://ec.europa.eu/health/ph_risk/committees/04_scenihr/docs/scenihr_o_003b.pdf⟩, European Commission Web, cited 14 November, 2010.
2) Scientific Committee on Emerging and Newly Identified Health Risks, SCENIHR: ⟨http://ec.europa.eu/health/ph_risk/committees/04_scenihr/docs/scenihr_o_010.pdf⟩, European Commission Web, cited 14 November, 2010.
3) Food Safety Authority of Ireland, FSA, "The Relevance for Food Safety of Applications of Nanotechnology in Food and Feed Industries," Dublin, 2008.
4) UK Committees on Toxicity, Mutagenicity and Carcinogenicity of Chemicals in Food, Consumer Products and the Environment (COT, COM, COC): ⟨http://cot.food.gov.uk/pdfs/cotstatements2005nanomats.pdf⟩, COT Web, cited 14 November, 2010.
5) The Committee on Toxicity of Chemicals in Food, Consumer Products and the Environment: ⟨http://www.food.gov.uk/multimedia/pdfs/cotstatementnanomats200701.pdf⟩, cited 14 November, 2010.
6) Takagi A., Hirose A., Nishimura T., Fukumori N., Ogata A., Ohashi N., Kitajima S., Kanno J., *J. Toxicol. Sci.*, **33**, 105–116 (2008).
7) Sakamoto Y., Nakae D., Fukumori N., Tayama K., Maekawa A., Imai K., Hirose A., Nishimura T., Ohashi N., Ogata A., *J. Toxicol. Sci.*, **34**, 65–76 (2009).
8) Xu J., Futakuchi M., Iigo M., Fukamachi K., Alexander D. B., Shimizu H., Sakai Y., Tamano S., Furukawa F., Uchino T., Tokunaga H., Nishimura T., Hirose A., Kanno J., Tsuda H., *Carcinogenesis*, **31**, 927–935 (2010).
9) Wako K., Kotani Y., Hirose A., Doi T., Hamada S., *J. Toxicol. Sci.*, **35**, 437–446 (2010).
10) Nurkiewicz T. R., Porter D. W., Hubbs A. F., Stone S., Chen B. T., Frazer D. G., Boegehold M. A., Castranova V., *Toxicol. Sci.*, **110**, 191–203 (2009).
11) Ryman-Rasmussen J. P., Cesta M. F., Brody A. R., Shipley-Phillips J. K., Everitt J. I., Tewksbury E. W., Moss O.R., Wrong B. A., Dodd D. F., Andersen M. E., Bonner J. C., *Nat. Nanotechnol.*, **4**, 747–751 (2009).
12) Shvedova A. A., Kishin E. R., Mercer R., Murray A. R., Johnson V. J., Potapovich A. I., Tyurina Y. Y., Gorelik O., Arepalli S., Schwegler-Berry D., Hubbs A. F., Antonini J., Evans D. E., Ku B. K., Ramsey D., Maynard A., Kagan V. E., Castranova V., Baron P., *Am. J. Physiol. Lung cell. mol. physiol.*, **289**, L698–L708 (2005).
13) Li Z., Hulderman T., Salmen R., Chapman R., Leonars S. S., Young S. H., Shvedova A., Luster M. I., Simeonove P. P., *Environ. Health Perspect.*, **115**, 377–382 (2007).
14) Nemmar A., Hoet P. H., Vandervoort P., Dinsdale D., Nemery B., Hoylaerts M. F., *J. Thromb. Haemost.*, **5**, 1217–1226 (2007).
15) Park E. J., Cho W. S., Jeong J., Yi J., Choi K., Park K., *Toxicology*, **259**, 113–121 (2009).
16) Nygaard U. C., Hansen J. S., Samuelsen M., Alberg T., Marioara C. D., Løvik M., *Toxicol. Sci.*, **109**, 113–123 (2009).
17) Inoue K., Koike E., Yanagisawa R., Hirano S., Nishikwa M., Takano H., *Toxicol. Appl. Pharmacol.*, **237**, 306–316 (2009).

The Journal of Toxicological Sciences (J. Toxicol. Sci.)
Vol.37, No.1, 81-89, 2012

Original Article

Teratogenicity of multi-wall carbon nanotube (MWCNT) in ICR mice

Tomoko Fujitani[1], Ken-ichi Ohyama[1], Akihiko Hirose[3], Tetsuji Nishimura[4], Dai Nakae[2] and Akio Ogata[1]

[1]Departments of Environmental Health and Toxicology and [2]Departments of Pharmaceutical Sciences, Tokyo Metropolitan Institute of Public Health, 3-24-1, Hyakunincho, Shin'juku, Tokyo 169-0073, Japan
[3]Divisions of Risk Assessment, Biological Safety Research Center and [4]Divisions of Environmental Chemistry, National Institute of Health Sciences, 1-18-1, Kamiyohga, Setagaya, Tokyo 158-8501, Japan

(Received July 21, 2011; Accepted November 8, 2011)

ABSTRACT — A possible teratogenicity of multi-wall carbon nanotube (MWCNT) was assessed using ICR mice. MWCNTs were suspended in 2% carboxymethyl cellulose and given intraperitoneally or intratracheally to pregnant ICR mice on day 9 of the gestation. All fetuses were removed from the uterus on day 18 of the gestation, and were examined for external and skeletal anomalies. In the intraperitoneal study, various types of malformation were observed in all MWCNT-treated groups (2, 3, 4 and 5 mg/kg body weight, intraperitoneal). In contrast, such malformations were observed in groups given 4 or 5 mg/kg body weight, but not in that treated with 3 mg/kg in the intratracheal study. In either study, the number of litters having fetuses with external malformation and that of litters having fetuses with skeletal malformations were both increased in proportion to the doses of MWCNT. The present results are the first to report that MWCNT possesses the teratogenicity at least under the present experimental conditions. Mechanism(s) to result such malformations is yet unclear and further experiment is necessary.

Key words: Multi-wall carbon nanotube, Nanomaterial, Teratogenicity, Hazard identification, Mice

INTRODUCTION

Carbon nanotube is a new form of the technological crystalline carbon and one of the most anticipated nanomaterials, because of its unique properties suitable for a variety of industrial products such as high strength materials, electronics and biomedical apparatuses (Martin and Kohli, 2003; Scott, 2005). On the other hand, potential hazards and/or risk for humans of carbon nanotube has been concerned, and large efforts have been internationally being made to investigate and evaluate them (Lam *et al.*, 2006; Pacurari *et al.*, 2010; Hubbs *et al.*, 2011). Among those, a possible carcinogenicity has been concerned most, assuming the structural similarity between carbon nanotubes and asbestos. Takagi *et al.* (2008) have first reported that multi-wall carbon nanotube (MWCNT) induces mesotheliomas, when intraperitoneally administered to male p53 gene deficient mice. Shortly afterwards, Sakamoto *et al.* (2009) have demonstrated that the carcinogenicity of MWCNT is a universal event and not specific to mice or genetically modified animals, by showing the mesothelioma development in male intact (not genetically modified) rats, intrascrotally administered the same MWCNT. Since then, carcinogenicity of MWCNT has enthusiastically been being studied but the mechanism(s) of such carcinogenicity is yet not clearly understood. Because the damage to DNA, directly or indirectly, by MWCNT is to be evaluated by prenatal stage, a possible teratogenicity must be another big issue for the risk assessment of MWCNT. To the best of our knowledge there have been no reports dealing with this issue in the literature. In this content, the present study was conducted to assess a possible teratogenicity of MWCNT.

MATERIALS AND METHODS

Ethical consideration of the experiments

An experimental protocol was approved by the Experiments Regulation Committee and the Animal Experiment Committee of the Tokyo Metropolitan Institute of Public Health prior to its execution and monitored at every step during the experimentation for its scientific and ethical appropriateness, including concern for animal welfare, with strict obedience to the National Institutes of Health Guideline for the Care and Use of Laboratory Animals, Japanese Government Animal Protection and Management Law, Japanese Government Notification on Feeding and Safekeeping of Animals and other similar laws, guidelines, rules and *et cetera* provided domestically and internationally.

Correspondence: Tomoko Fujitani (E-mail: Tomoko_Fujitani@member.metro.tokyo.jp)

Animals

Specific pathogen free Crlj:CD1(ICR) mice, 5 weeks old, were purchased from Charles River Japan Inc., Kanagawa, Japan and were sufficiently acclimatized before use. Mice were housed individually in plastic cage (180 x 305 x 110mm^3) with cedar chip bedding and free access to the standard diet CE2 (Nihon Clea, Inc., Tokyo, Japan) and water. The animal room was maintained at 23-25°C with a relative humidity of 50-60%, with 10 ventilation per hour (drawing fresh air through an HEPA-filter, 0.3 μm, 99.9% efficiency) and on a 12 hr light/dark cycle. At 8 to 13 weeks old, a nulliparous female was housed overnight with a male and the next morning the female was checked for the presence of a vaginal plug. The day when vaginal-plug formation was observed was regarded as day 0 of the gestation.

Test chemicals

The presently utilized test chemicals, MWCNT (MITSUI MWCNT-7; lot number, 060125-01k) was exactly identical to those used in the carcinogenicity studies in *p53* gene deficient mice (Takagi *et al.*, 2008) and in intact rats (Sakamoto *et al.*, 2009). MWCNT was suspended in 2% carboxymethyl cellulose sodium (CMCNa; Tokyo Chemical Industry Co., Ltd., Tokyo, Japan) solution at concentrations of 0.2, 0.3, 0.4 or 0.5 mg/ml for the intraperitoneal study to achieve a uniform administration volume of 10 ml/kg body weight. In the case of the intratracheal study, 3, 4 and 5 mg/ml suspensions were prepared to achieve a uniform administration volume of 1 ml/kg. The control (0 mg/kg body weight) animals were received 2% CMCNa solution, intraperitoneally or intratracheally, respectively. These suspensions as well as a vehicle 2% CMCNa solution were sterilized by an autoclave at 120°C for 20 min and vigorously mixed by hand shaking immediately prior to the administration.

Animal treatment and assessments

Two independent experiments were performed. In experiment 1, pregnant female mice were given a single intraperitoneal administration of MWCNT at dosages of 2, 3, 4 or 5 mg/kg body weight on day 9 of the gestation. On the other hand, in experiment 2, mice were given a single intratracheal spray administration of 3, 4 or 5 mg/kg body weight using intratracheal aerosolizer (MicroSprayer Model IA-1B; Penn-Century, Inc., Philadelphia, PA, USA) on day 9 of the gestation.

In either experiment, body weights of mated females were measured daily, and clinical observations were recorded. All mice were killed on day 18 of the gestation under light ether anesthesia. The liver, lung, spleen, heart, kidney, thymus and tracheobronchial lymph node of each dam were removed and weighed. Peripheral blood was examined for the leukocyte counting by Sysmex KX-21NV. Blood films were made, stained by May/Grünwald;Giemsa and counted for the subtypes of leucocytes under the light microscopy.

The uterus was opened to examine for early and late fetal deaths, and to record the position of dead and live fetuses. The numbers of implantation sites and corpora lutea in the ovaries were also counted. Each live fetus was weighed and examined for external anomalies. Fetuses were fixed in 95% ethanol and stained with Alizarin Red S (Dawson, 1926) to examine skeletal anomalies.

Statistical analysis

Scheffe's multiple comparison was applied for the organ weights of dams, maternal body weights, number of implantations and live fetuses, and fetal body weights. The incidence of pregnant females and of litters with malformed fetuses, and the number of malformed fetuses were analyzed using the Chi square test. The rank sum test was used for data on the resorption and the percent incidence of malformations (Nishimura, 1976). The trend test (cumulative X2 test) was performed to evaluate the significance of the development of malformations by the administered doses of MWCNT.

RESULTS

Experiment 1, the intraperitoneal study

The pregnant status is summarized in Table 1. No animals died after the MWCNT administration. While most of the mated mice were gestated regardless to treatments, 1, 1, 6 and 6 pregnant mice, which were dosed 2, 3, 4 and 5 mg/kg body weight of MWCNT respectively, did not have any living fetuses on 18 day of the gestation. The statistical significances of this change were obtained in the 4- and 5-mg/kg groups. Similarly, the rates of early resorption of fetuses were significantly increased, with the number of live fetuses per litter being decreased, in these groups. In addition, the body weights of live fetuses were significantly lower in the 2-, 3- and 4-mg/kg groups,

Table 1. Experiment 1; pregnant status

Reproductive parameters	MWCNT dose (mg/kg body weight)				
	0 (control)	2	3	4	5
Female mated[1)]	11	12	12	15	10
Female died[2)]	0	0	0	0	0
Female gestated[3)]	10	8	9	13	9
Female with >1 live fetus	10	7	8	7*	3**
Corpora lutea/litter[#]	15.8 ± 1.9	15.6 ± 1.6	16.0 ± 4.1	15.4 ± 1.8	14.4 ± 2.2
Implantations/litter[#]	14.5 ± 2.5	14.4 ± 1.5	12.3 ± 2.7	14.0 ± 2.1	12.7 ± 3.8
Resorption of fetuses(%)[4)#]					
Early	11.0 ± 13.5	35.3 ± 34.9	41.7 ± 34.8	67.1 ± 38.8**	81.7 ± 28.2***
Late	1.7 ± 3.7	2.4 ± 3.4	0	1.6 ± 3.1	0.9 ± 2.6
Live fetus /litter[#]	12.6 ± 2.6	9.5 ± 5.1	7.3 ± 4.1	4.8 ± 5.8**	1.4 ± 3.3***
Body wt of live fetus (g) [#]					
Male	1.48 ± 0.10	1.29 ± 0.08*	1.28 ± 0.10**	1.31 ± 0.08*	1.42 ± 0.12
Female	1.43 ± 0.13	1.23 ± 0.09*	1.24 ± 0.12*	1.21 ± 0.11*	1.33 ± 0.02

[1)] Number of animals with vaginal plug. [2)] Number of animals died before the scheduled sacrifice on day 18 of the gestation. [3)] Number of animals with implantation sites. [4)] 'Early' was defined as a case showing the implanted sites and amorphous mass, while 'Late' was defined as a case showing the head and limbs. [#] Values are the means ± S.D. The percent resorption and foetal body weight were obtained by averaging the value for each litter. Asterisks represent that the values are significantly different from the control value (*, ** or *** indicating $p < 0.05$, 0.01 or 0.001, respectively).

but not in the 5-mg/kg group, than in the control group.

Figure 1 illustrates changes of the maternal body weight, of which increment was retarded by MWCNT with a dose-dependent tendency. The body and organ weights and leucocyte typing and counting data of dams are summarized in Table 2. The final body weights were significantly decreased in the 4- and 5-mg/kg groups. The liver weight tended decreased in the dose groups but changes were not statistically significant. The weight of the spleen was significantly increased in the dose groups but no other adverse effect was evident. The numbers of total white blood cells, neutrophils, eosinophils and monocytes, lymphocytes as well but lesser degree, all tended increased in all MWCNT-treated groups. The statistical significances of these changes were obtained in the 3-mg/kg group for the total white blood cells and in 2- 3- and 4-mg/kg groups for the neutro- and eosinophils.

The incidences of malformations were summarized in Table 3. Various types of external and skeletal malformations, such as reduction deformity of limb, short or absent tail, cleft palate, fusion of vertebrae, hypophalangia and hyperphalangia, were observed not in the control group but in all MWCNT-treated groups. Whereas respective incidences of such malformations were a few, the ratio of litters with malformed fetuses, the percent incidence of malformations and the ratio of malformed fetuses were all increased in all MWCNT-treated groups, most of them being with the statistical significance. The trend test evaluated that the development of skeletal malformations by the administered doses of MWCNT was significant ($p < 0.05$).

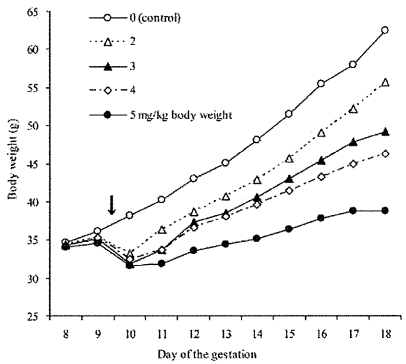

Fig. 1. Experiment 1; changes of the maternal body weights. The arrow represents the timing of the intraperitoneal administration of MWCNT.

Table 2. Experiment 1; body and organ weights, and leucocyte typing and counting of dams

Items	MWCNT dose (mg/kg body weight)				
	0 (control)	2	3	4	5
Number of dam	10	8	9	13	9
Body weight on day 9 of the gestation	36.1 ± 1.3	35.3 ± 1.9	35.2 ± 2.9	35.2 ± 2.6	34.6 ± 2.4
on day 18 of the gestation	62.4 ± 2.8	55.7 ± 12.0	49.2 ± 7.9	46.3 ± 11.9*	38.8 ± 9.4***
Organ weight					
Liver (g)	3.11 ± 0.40	3.17 ± 0.53	2.99 ± 0.49	2.80 ± 0.52	2.42 ± 0.64
Kidney (mg)	478 ± 133	503 ± 52	447 ± 48	472 ± 55	452 ± 55
Heart (mg)	179 ± 17	180 ± 23	167 ± 18	165 ± 16	157 ± 22
Lung (mg)	189 ± 8	181 ± 3	176 ± 20	188 ± 15	202 ± 20
Spleen (mg)	145 ± 40	297 ± 88*	323 ± 86**	333 ± 99**	372 ± 91***
Thymus (mg)	26.6 ± 12.9	22.6 ± 5.4	17.2 ± 9.2	25.3 ± 7.4	37.8 ± 15.0
Tracheobronchial lymph node (mg)	7.4 ± 8.3	7.3 ± 3.5	8.8 ± 4.5	6.2 ± 4.5	14.6 ± 5.1
Leucocyte count (10^2/μl)					
Total	47 ± 19	115 ± 34	124 ± 48*	109 ± 68	82 ± 38
Lymphocyte	28.9 ± 11.7	38.8 ± 12.0	33.6 ± 15.1	33.0 ± 35.7	23.9 ± 11.4
Neutrophil	15.0 ± 7.0	54.6 ± 19.2*	66.1 ± 23.0**	53.6 ± 37.0*	46.5 ± 23.9
Eosinophil	0.9 ± 0.5	17.5 ± 14.1**	16.1 ± 8.9**	15.5 ± 8.1**	6.7 ± 5.0
Monocyte	1.9 ± 1.7	4.1 ± 3.0	8.2 ± 7.8	7.0 ± 4.2	5.5 ± 4.0

Values are the mean ± S.D. Asterisks represent that the values are significantly different from the control value (*, ** or *** indicating $p < 0.05$, 0.01 or 0.001, respectively).

Table 3. Experiment 1; incidences of malformations

Items	MWCNT dose (mg/kg body weight)				
	0 (control)	2	3	4	5
External malformation					
Numbers of litters with malformed fetuses/examined (percentages in the parentheses)					
	0/10(0)	2/7(28.6)	2/8(25.0)	3/7(42.9)*	1/3(33.3)
Percent incidence of malformations[#]	0	9.2 ± 18.8	3.6 ± 6.8	4.6 ± 6.5	6.7 ± 11.5
Numbers of malformed fetuses/examined	0/126	3/76*	3/66*	3/63*	2/13***
Numbers of fetuses with					
short or absent tail	0	2	1	1	0
cleft palate	0	0	0	1	0
reduction deformity of limb	0	2	3	1	2
Skeletal malformation					
Numbers of litters with malformed fetuses/examined (percentages in the parentheses)					
	0/10(0)	4/7(57.1)**	3/8(37.5)*	3/7(42.9)*	2/3(66.7)**
Percent incidence of malformations[#]	0.0 ± 0.0	14.4 ± 18.1	11.1 ± 21.7	11.9 ± 19.2	40.0 ± 52.9
Numbers of malformed fetuses/examined	0/126	9/76***	7/66***	7/63***	5/13***
Numbers of fetuses with					
fusion of ribs	0	3	1	2	0
fusion of vertebral bodies and arches	0	6	7	0	3
hypophalangia	0	2	2	3	2
hyperphalangia	0	0	0	2	0

[#]Calculated by averaging the percentage in each litter (*i.e.* numbers of malformations/fetuses) and shown as the means ± S.D. Asterisks represent that the values are significantly different from the control value (*, ** or *** indicating $p < 0.05$, 0.01 or 0.001, respectively).

Experiment 2, the intratracheal study

The pregnant status is summarized in Table 4. No animals died after the MWCNT administration. Most of the treated mated mice were gestated, and all of them had living fetuses. The rates of early as well as late resorption of fetuses were increased in the 4- and 5-mg/kg groups, respectively, but these changes were not statistically significant because of a large dispersion. The numbers of live fetuses per litter in MWCNT-treated groups were well maintained, although slight decreases were seen in the 4- and 5-mg/kg groups. In contrast, the body weight of live fetuses was significantly lower in the 5-mg/kg group.

Figure 2 illustrates changes of the maternal body weights, of which increment was retarded in the 5-mg/kg group. The body and organ weights, and leucocyte typing and counting data of dam are summarized in Table 5. The final body weight was significantly decreased in the 5-mg/kg group. The weight of the lung and tracheobronchial lymph nodes tended increased in a dose-dependent tendency, and the statistical significance was achieved for the lung in the 5-mg/kg group. Lungs of dosed groups looked blackened. The numbers of total white blood cells tended increased in a dose-dependent tendency, and the statistical significance was achieved in the 4- and 5-mg/kg group, but the magnitude of this change was not so high. The numbers of all types of white blood cell looked increased in some MWCNT-treated group, but the changes were modest and lacked statistical significances.

The incidences of malformations were summarized in Table 6. Various types of external and skeletal malformations, as seen in experiment 1, were observed not in the control group and scarcely in the 3-mg/kg group. In the 4- and 5-mg/kg groups, however, such malformations occurred frequently and significantly. Typical features of the reduction deformity of limb and the fusion of vertebrae and ribs are demonstrated in Figs. 3 and 4, respectively. The ratio of litter with malformed fetuses, the percent incidence of malformations and the ratio of malformed fetuses were all increased in 4- and 5-mg/kg group, most of them being with the statistical significance.

DISCUSSION

The present results clearly elicit that MWCNT is teratogenic in mice, at least under the present experimental conditions. This is the first report demonstrate the teratogenicity of this nanomaterials. Also, there is no report on teratogenicity of other exogenous fibers such as single wall nanotubes, asbestos and glass fibers. It is sometimes difficult to judge teratogenicities of chemicals, especially when the maternal toxicity is present. Because the maternal toxicity was in fact observed in some MWCNT-treated groups of the present study, one might consider the malformation of the fetuses only reflected and thus did not necessarily indicate the "true" teratogenicity of MWC-

Table 4. Experiment 2; pregnant status

Reproductive parameter	MWCNT dose (mg/kg body weight)			
	0 (control)	3	4	5
Female mated[1)]	11	12	16	6
Female died[2)]	0	0	0	0
Female gestated[3)]	10	10	15	5
Female with >1 live fetus	10	10	15	5
Corpora lutea/litter	14.6 ± 1.5	16.0 ± 1.8	15.1 ± 1.8	15.8 ± 2.3
Implantations/litter	12.8 ± 1.6	14.8 ± 2.2	13.8 ± 2.7	11.8 ± 2.9
Resorption of fetuses(%) [4)#]				
Early	9.8 ± 13.4	8.8 ± 8.4	21.0 ± 29.8	20.0 ± 17.7
Late	2.0 ± 4.6	0.6 ± 1.8	0.8 ± 2.2	6.3 ± 10.1
Live fetus/litter[#]	11.3 ± 2.1	13.3 ± 1.5	10.5 ± 4.4	8.8 ± 2.9
Body weight of live fetus (g) [#]				
Male	1.41 ± 0.14	1.36 ± 0.12	1.23 ± 0.19	1.07 ± 0.20*
Female	1.35 ± 0.13	1.31 ± 0.11	1.19 ± 0.19	1.06 ± 0.18*

[1)] Number of animals with vaginal plug. [2)] Number of animals died before the scheduled sacrifice on day 18 of the gestation. [3)] Number of animals with implantation sites. [4)] 'Early' was defined as a case showing the implanted sites and amorphous mass, while 'Late' was defined as a case showing the head and limbs. [#] Values are the means ± S.D. The percent resorption and fetal body weight were obtained by averaging the value for each litter. Asterisks represent that the values are significantly different from the control value (* indicating $p < 0.05$).

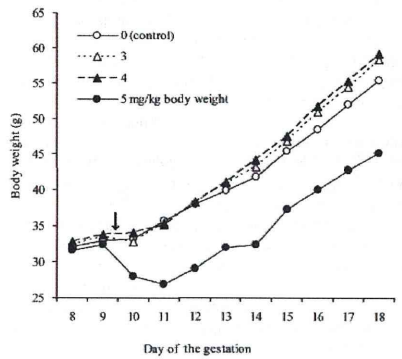

Fig. 2. Experiment 2; changes of the maternal body weights. The arrow represents the timing of the intratracheal administration of MWCNT.

Fig. 3. Experiment 2; an 18-day-old fetus, showing the reduction deformity of the limb, from a dam intratracheally administered MWCNT at a dose of 4 mg/kg body weight on day 9 of the gestation.

NT. Malformations were, however, induced even in the 4-mg/kg group of the intratracheal study, in which MWCNT did not apparently cause the maternal toxicity. In addition, the malformations induced by the MWCNT administration belonged to a reduction type, such as the reduction

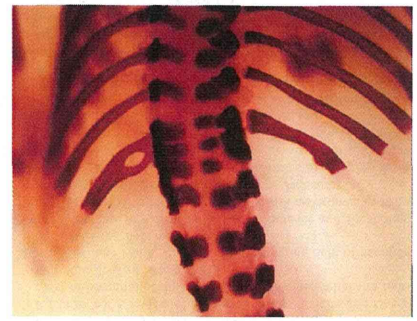

Fig. 4. Experiment 2; an 18-day-old fetus, showing the fusion of vertebrae and ribs, from a dam intratracheally administered MWCNT at a dose of 4 mg/kg body weight on day 9 of the gestation.

deformity of limbs and the short or absent tail. The malformations in this type have not been found among about 7,000 fetuses of ICR mice historically examined so far in our laboratory (Ogata *et al.*, 1984, 1987, 1989 and 1999). Also in other laboratories, the spontaneous incidence of the reduction deformity of limb of ICR mice is usually very low. For instance, the incidence of amelia and oligoductilia has both been reported to be 0.02% among 5,000 fetuses in another laboratory and no deformities have observed among 4,335 fetuses in another laboratory (Kameyama *et al.*, 1980). The malformations observed in this study are uncommon in merely by the maternal toxicity. It is thus safe to say that the teratogenicity of MWCNT demonstrated in the present study is true with a biological significance.

The reasons why we at first conducted the intraperitoneal study and used very high doses were to avoid missing a teratogenicity of MWCNT, if it is present, under the experimental condition as sensitive as possible form the point of the hazard identification. This is the same strategy that was adopted in the studies identifying the carcinogenic hazard of MWCNT (Sakamoto *et al.*, 2009; Takagi *et al.*, 2008). The relatively severe maternal toxicity in the high doses is thus rather expected. Nevertheless, the present intraperitoneal study can demonstrate the teratogenicity of MWCNT as stated above, witch then led us to confirm this hazard using a more human-relevant exposure route. In the intratracheal study, MWCNT was administered into the trachea of mice in a spray or mist shape, witch well mimics the most plausible human

Table 5. Experiment 2; body and organ weights, and leucocyte typing and counting of dams

Items	MWCNT dose (mg/kg body weight)			
	0 (control)	3	4	5
Number of dam	10	10	15	5
Body weight on day 9 of the gestation	33.0 ± 2.0	33.6 ± 2.8	33.8 ± 2.8	32.5 ± 2.2
on day 18 of the gestation	55.4 ± 3.1	58.4 ± 5.5	59.1 ± 6.9	45.1 ± 4.5*
Organ weight				
Liver (g)	2.80 ± 0.27	2.73 ± 0.36	3.05 ± 0.31	2.44 ± 0.11
Kidney (mg)	454 ± 52	431 ± 60	457 ± 54	422 ± 28
Heart (mg)	155 ± 10	161 ± 14	162 ± 15	150 ± 9
Lung (mg)	157 ± 14	168 ± 10	197 ± 51	228 ± 47**
Spleen (mg)	136 ± 22	122 ± 29	149 ± 40	158 ± 35
Thymus (mg)	19.9 ± 7.5	16.4 ± 5.3	18.9 ± 5.5	13.9 ± 8.9
Tracheobronchial lymph node (mg)	4.2 ± 3.6	6.8 ± 5.2	6.2 ± 4.3	8.7 ± 2.3
Leucocyte count (10^2/μl)				
Total	37.5 ± 6.4	49.5 ± 11.3	51.6 ± 11.5*	51.3 ± 10.6*
Lymphocyte	21.0 ± 4.4	30.0 ± 8.2	26.5 ± 7.4	22.5 ± 6.4
Neutrophil	14.7 ± 4.5	17.4 ± 9.7	20.3 ± 11.2	25.4 ± 11.5
Eosinophil	0.7 ± 0.9	1.1 ± 0.7	2.7 ± 2.5	1.6 ± 1.1
Monocyte	1.2 ± 0.7	1.0 ± 0.5	2.2 ± 1.4	1.7 ± 0.4

Values are the means ± S.D. Asterisks represent that values are significantly different from the control value (* or ** indicating $p < 0.05$ or 0.01, respectively).

Table 6. Experiment 2; incidences of malformations

Items	MWCNT dose (mg/kg body weight)			
	0 (control)	3	4	5
External malformation				
Number of litters with malformed fetuses/examined (percentages in the parentheses)				
	0/10(0)	0/10(0)	5/14(35.7)*	2/5(40.0)*
Percent incidence of malformations[#]	0	0	15.6 ± 27.9	5.6 ± 8.2
Number of malformed fetuses/examined	0/113	0/133	15/158***	3/44**
Number of fetuses with				
short or absent tail	0	0	12**	3**
reduction deformity of limb	0	0	7*	0
Skeletal malformation				
Number of litters with malformed fetuses/examined (percentages in the parentheses)				
	0/10(0)	1/10(10.0)	6/14(42.8)*	4/5(80.0)*
Percent incidence of malformations[#]	0	0	39.9 ± 48.4*	61.9 ± 38.2*
Number of malformed fetuses/examined	0/113	1/133	56/158***	31/44***
Number of fetuses with				
fusion of ribs	0	0	8*	10***
fusion of vertebral bodies and arches	0	0	54***	25***
hypophalangia	0	0	10*	1
hyperphalangia	0	1	0	1

[#] Calculated by averaging the percentage in each litter (*i.e.*, number of malformations/fetuses) and shown as the means ± S.D. Asterisks represent that the values are significantly different from the control value (*, ** or *** indicating $p < 0.05$, 0.01 or 0.001, respectively).

exposure situation of the inhalation. The highest dose of 5 mg/kg body weight must have been too high, because it caused the apparent maternal toxicity, and it agglomerated in the lung (data not shown). It is clearly indicated, however, that MWCNT is teratogenic, because the malformations in the fetuses were significantly induced by the middle dose of 4 mg/kg body weight that did not cause the apparent maternal toxicity.

It is known that methyl cellulose of a certain length has nephrotoxicity but, in this study, no adverse effect on kidney of dam given 2% CMCNa solution (control) nor suspension of MWCNT in 2% CMCNa (dosed groups) was observed.

Mechanisms underlying the teratogenicity of MWCNT are still obscure. Sargent *et al.* (2009) has demonstrated that single-wall carbon nanotube induces aneuploidy in cultures primary and immortalized human airway epitherial cells by the disruption of the mitotic spindle. In that study, the association of nanotubes with cellular and mitotic tubulins as well as chromatins within the nuclei is demonstrated, and the similarity of nanotube bundles to microtubules in size of microtubules is considered to play roles, because it may make nanotubes incorporated into the mitotic spindle apparatus. Recently, Takahashi *et al.* (2010) has reported that MWCNT also induces polyploidy, suggesting that MWCNT may exert similar effects on microtubules to the situation of single-wall carbon nanotube. If it is a case, the disruption of the mitotic spindle and the fragmentation of the centrosomes may inhibit subsequent cell division, which results in the embryonic death in early phase and the malformation of the reduction type. Further studies are apparently warranted, and especially a passage of MWCNT through the placenta and the reach to the fetus should be evidenced.

Another possible factor involved in the teratogenicity may be the chronically persisting inflammation caused by the exposure to MWCNT, which is frequently considered to participate in the biological effects of nanomaterials (Takagi *et al.*, 2008; Sakamoto *et al.*, 2009; Erdely *et al.*, 2009; Hubbs *et al.*, 2011). The present results of the increments of the numbers of leucocyte and related hemocytes, and of the weight of the spleen might support this possibility.

The present intratracheal study gives no-observed-adverse-effect level (NOAEL) of 3 mg/kg body weight for external and skeletal malformations. Although the human exposure level of MWCNT has not as yet clearly determined, the interim report for the risk assessment of MWCNT by the National Institute of Advanced Industrial Science and Technology (AIST, 2009) roughly estimated the quantity of MWCNT exposure of workers as 0.53- 6.20 μg/kg/day. Comparing with these values, the above NOAEL for external and skeletal malformations are approximately 480-5,660 times high. It is thus tentatively evaluated that the present results may not necessarily or immediately indicate a human risk. Needless to say, however, more detailed and careful investigations including those for the teratogenicity must be conducted to complete the risk assessment of MWCNT.

ACKNOWLEDGMENTS

This work was supported in part by a research budget of the Tokyo Metropolitan Government, Japan, and a Grant-in-Aid from the Ministry of Health, Labor and Welfare of Japan. Authors gratefully thank to Mr. Ando, Mr. Kubo, Mr. Yano, Mr. Takahashi, Mr. Yuzawa and Mr. Nagasawa, for their technical assistance.

REFERENCES

Dawson, A.B. (1926): A note on the staining of the skeleton of cleared specimens with Alizarin Red S. Stain Techno., **1**, 123-124.

Erdely, A., Hulderman, T., Salmen, R., Liston, A., Zeidler-Erdely, P.C., Schwegler-Berry, D., Castranova, V., Koyama, S., Kim, Y.-A., Endo, M. and Simeonova, P.P. (2009): Cross-talk between lung and systemic circulation during carbon nanotube respiratory exposure. Potential biomarkers. Nano Letters, **9**, 36-43.

Hubbs, A.F., Mercer, R.R., Benkovic, S.A., Harkema, J., Sriram, K., Schwegler-Berry, D., Goravanahally, M.P., Nurkiewicz, T.R., Castranova, V. and Sargent, L.M. (2011): Nanotoxicology--A pathologist's Perspective. Toxicol. Pathol., **39**, 301-324.

Kameyama, Y., Tanimura, T. and Yasuda, M. (1980): Spontaneous malformations in laboratory animals : Photographic atlas and reference data. Congenital Anomalies, **20**, 25-106. (in Japanese).

Lam, C.-W., James, J.T., McCluskey, R., Arepalli, S. and Hunter, R.L. (2006): A review of carbon nanotube toxicity and assessment of potential occupational and environmental health risks. Crit. Rev. Toxicol., **36**, 189-217.

Martin, C.R. and Kohli, P. (2003): The emerging field of nanotube biotechnology. Nat. Rev. Drug Discov., **2**, 29-37.

National Institute of Advanced Industrial Science and Technology (AIST) (2009): The interim report--the risk assessment of nanomaterials (CNT)--Executive summary. (in Japanese).

Nishimura, H. (1976): Could skin applications of cleaning detergents be teratogenic? Course of the successive joint studies and interpretation of the results. Congenital Anomalies, **16**, 175-185. (in Japanese).

Ogata, A., Ando, H., Kubo, Y. and Hiraga, K. (1984): Teratogenicity of thiabendazole in ICR mice. Food Chem. Toxicol., **22**, 509-520.

Ogata, A., Yoneyama, M., Sasaki, M., Suzuki, K. and Imamichi, T. (1987): Effects of pretreatment with SKF-525A or sodium phenobarbital on thiabendazole-induced teratogenicity in ICR mice. Food Chem. Toxicol., **25**, 119-124.

Ogata, A., Fujitani, T., Yoneyama, M., Sasaki, M. and Suzuki, K. (1989): Glutathione and cysteine enhance and diethylmaleate reduces thiabendazole teratogenicity in mice. Food Chem.

Toxicol., **27**, 117-123.
Ogata, A., Ando, H., Kubo, Y., Nagasawa, A., Ogawa, H., Yasuda, K. and Aoki, N. (1999): Teratogenicity of thujaplicin in ICR mice. Food Chem. Toxicol., **37**, 1097-1104. Erratum in Food Chem. Toxicol., 2000, **38**, 125.
Pacurari, M., Castranova, V. and Vallyathan, V. (2010): Single- and multi-wall carbon nanotubes versus asbestos: Are the carbon nanotubes a new health risk to humans? J. Toxicol. Environ. Health Part A, **73**, 378-395.
Sakamoto,Y., Nakae, D., Fukumori, N., Tayama, K., Maekawa, A., Imai, K., Hirose, A., Nishimura, T., Ohashi, N. and Ogata, A.(2009): Induction of mesothelioma by a single intrascrotal administration of multi-wall carbon nanotube in intact male Fischer 344 rats. J. Toxicol. Sci., **34**, 65-76.
Sargent, L.M., Shvedova, A.A., Hubbs, A.F., Salisbury, J.L., Benkovic, S.A., Kashon, M.L., Lowry, D.T., Murray, A.R., Kisin, E.R., Friend, S., McKinstry, K.T., Battelli, L. and Reynolds, S.H. (2009): Induction of aneuploidy by single-walled carbon nanotubes. Environ. Mol. Mutagen., **50**, 708-717.
Scott, N.R. (2005): Nanotechnology and animal health. Rev. Sci. Tech., **24**, 425-432.
Takagi, A., Hirose, A., Nishimura, T., Fukumori, N., Ogata, A., Ohashi, N., Kitajima, S. and Kanno, J. (2008): Induction of mesothelioma in p53+/- mouse by intraperitoneal application of multi-wall carbon nanotube. J. Toxicol. Sci., **33**, 105-116.
Takahashi, T., Asada, S., Hara, T., Toyoizumi, T., Saitoh, Y., Kumagai, H., Yamakage, K. and Honma, M (2010): Chromosomal aberration test of multi-wall carbon nanotubes (MWCNT) using CHL/IU cells. 39th Annual Meeting of the Japanese Environmental Mutagen Society, Program abstract.

The Journal of Toxicological Sciences (J. Toxicol. Sci.)
Vol.37, No.1, 177-189, 2012

Original Article

Effects of sustained stimulation with multi-wall carbon nanotubes on immune and inflammatory responses in mice

Atsumi Yamaguchi[1], Tomoko Fujitani[1], Ken-ichi Ohyama[1], Dai Nakae[2], Akihiko Hirose[3], Tetsuji Nishimura[4], Akio Ogata[1]

[1]Departments of Environmental Health and Toxicology and [2]Departments of Pharmaceutical Sciences, Tokyo Metropolitan Institute of Public Health, 3-24-1 Hyakunin-cho, Shinjuku-ku, Tokyo 169-0073, Japan
[3]Divisions of Risk Assessment and [4]Divisions of Environmental Chemistry, National Institute of Health Science, 1-18-1 Kamiyoga, Setagaya-ku, Tokyo 158-8501, Japan

(Received October 19, 2011; Accepted December 5, 2011)

ABSTRACT — Possible effects of multi-wall carbon nanotubes (MWCNTs) on immune and inflammatory responses were examined in mice. Female ICR mice were given a single intraperitoneal administration (2 mg/kg body weight) of either MWCNTs, carbon black (CB), or crocidolite (blue asbestos) and controls received a vehicle of 2% sodium carboxymethyl cellulose (CMC Na). In the peritoneal cavity of MWCNT-administered mice, the liver had changed to a rounded shape and fibrous adhesions were seen on internal organs. Peritoneal cells overexpressed mRNA for genes of T helper (Th)2 cytokines (*interleukin [IL]-4*, *IL-5*, and *IL-13*), Th17 cytokine (*IL-17*), pro-inflammatory cytokines/chemokines (*IL-1β*, *IL-33*, *tumor necrosis factor α*, and *monocyte chemotactic protein-1*), and *myeloid differentiation factor 88* for at least 2 weeks after the administration of MWCNTs, while those of Th1 cytokine genes (*IL-2* and *interferon γ*) were overexpressed several weeks later and expression levels remained high up to 20 weeks. In MWCNT-treated mice, the numbers of leukocytes, monocytes, and granulocytes in the peripheral blood and the expression of the leukocyte adhesion molecules, cluster of differentiation (CD)49d and CD54, on granulocytes were increased 1 week after administration and remained high up to week 20. Production of ovalbumin-specific IgM and IgG_1 was enhanced by MWCNTs. These changes were not observed after CB or crocidolite administration. Thus, this study showed that MWCNTs exhibited sustained stimulating effects on immune and inflammatory responses, unlike the other mineral fibers with structural similarities.

Key words: Multi-wall carbon nanotube, Nanomaterial, Inflammation, Immunotoxicity, Hazard characterization

INTRODUCTION

Rapid progress in nanotechnology in recent years has made it possible to produce and apply numerous new and useful nanomaterials, such as nano-TiO_2, nano-SiO_2, nano-ZnO and nano-carbon materials. These are believed to be biologically inert, although inhalation of small-sized nanomaterials can cause pulmonary inflammation and fibrosis. (Mossman and Churg, 1998; Yazdi *et al.*, 2010). Carbon forms exist in many different shapes as both elementary substances and compounds, for example, diamond, charcoal, carbon black, graphite, fullerene, and carbon nanotubes are all carbon allotropes, while graphene is a single-wall product of graphite, whose structure consists of one-atom-thick planar sheets of hexagonal-bonded carbon atoms densely packed in honeycomb crystal lattices. Carbon nanotubes are seamless cylindrical structures comprising single or multiple graphene sheets. Both single-wall carbon nanotubes (SWCNTs) and multi-wall carbon nanotubes (MWCNTs) are several micrometers in length and approximately 1-20 nanometers in diameter. These needle-like structures resemble asbestos.

It is well known that asbestos inhalation causes pulmonary inflammation and fibrosis, lung cancer, and malignant mesothelioma after relatively long latency periods (Mossman *et al.*, 1990; Hei *et al.*, 1992). However, the signaling pathways that lead to the development of these asbestos-associated diseases remain largely unknown. If

Correspondence: Atsumi Yamaguchi (E-mail: Yamaguchi@member.metro.tokyo.jp)

carbon nanotubes can create the hazards and risks similar to those associated with asbestos, they must be appropriately assessed and managed to protect human health.

In vivo effects of MWCNTs have been studied using animal models with a variety of exposure methods, such as inhalation, intratracheal instillation, pharyngeal aspiration, and intraperitoneal injection, and their effects on inflammatory responses have been described. Mice exposed to MWCNTs by inhalation caused platelet-derived growth factor (PDGF) overexpression, inflammatory cell aggregation, and recruitment of macrophages that phagocytosed MWCNTs in the lung within 1 day, followed by the subsequent development of subpleural fibrosis during weeks 2-6 (Ryman-Rasmussen *et al.*, 2009a, 2009b). Pharyngeal aspiration of MWCNTs in mice caused the rapid development of fibrosis within 7 days and a persistent granulomatous inflammation throughout a 56-day post-exposure period (Porter *et al.*, 2010). Intratracheal instillation of MWCNTs in mice caused an increase in the number of neutrophils and the levels of cytokines in bronchoalveolar lavage (BAL) fluid within 1 day, and granulomatous lesions developed and persisted until day 14 of these experiments (Park *et al.*, 2009). Intraperitoneal injection of MWCNTs given to rats (Sakamoto *et al.*, 2009) or *p53* gene heterozygously deficient mice (Takagi *et al.*, 2008) induced a long-lasting inflammation and resulted in fibrous thickening and granuloma formation in the peritoneum in association with the induction of mesothelioma.

However, despite evidences from these studies, the potential immunotoxicity of MWCNTs has not been sufficiently established till date. Thus, the present study was conducted to assess a possible involvement of MWCNTs in immune and inflammatory responses of ICR mice. Intraperitoneal administration was chosen as the exposure route for MWCNTs. Although it may not be directly relevant to humans, intraperitoneal administration in a rodent model is sensitive enough to detect weak effects of MWCNTs, which was why this strategy was adopted to identify a possible carcinogenic hazard of MWCNTs (Sakamoto *et al.*, 2009; Takagi *et al.*, 2008). In addition, intraperitoneal administration can control and ensure the relationship between administration doses and agent exposure. Furthermore, some reports have clearly indicated the detection of inhaled MWCNTs in the subpleura (Ryman-Rasmussen *et al.*, 2009a), pharyngeally-aspirated MWCNTs in the pleura (Porter *et al.*, 2010), and intraperitoneally-administered MWCNTs in the liver and mesenteric lymph nodes (Sakamoto *et al.*, 2009). These results suggest that MWCNTs are distributed to a certain extent in the entire body, regardless of the exposure route used.

MATERIALS AND METHODS

Ethical approval

Our experimental protocols were approved by the Experiments Regulation Committee and the Animal Experiment Committee of the Tokyo Metropolitan Institute of Public Health prior to beginning of these experiments and were monitored at each step of experimentation for scientific and ethical appropriateness, including concerns for animal welfare, with strict adherence to the National Institutes of Health Guidelines for the Care and Use of Laboratory Animals, Japanese Government Animal Protection and Management Law, Japanese Government Notification on Feeding and Safekeeping of Animals, and other similar laws, guidelines, and rules provided domestically and internationally.

Animals

Specific pathogen-free female Crlj:CD1(ICR) mice, 6-7 weeks old, were purchased from Charles River Japan, Inc. (Kanagawa, Japan) and acclimatized for 1 week. Mice were housed individually in plastic cages (22 × 15 × 12 cm) with cedar chip bedding and had free access to a standard diet CE2 (Nihon Clea, Inc., Tokyo, Japan) and water. The animal room was maintained at 24°C-26°C with a relative humidity of 50%-60%, with 10 ventilations per hour (drawing fresh air through a high-efficiency particulate air filter, 0.3 μm, 99.9% efficiency), and on a 12 hr light/dark cycle.

Chemicals, reagents, and kits

MWCNTs (MITSUI MWCNT-7; lot number 060125-01k) were provided by National Institute of Health Science, Tokyo, Japan. These were exactly identical to those used in carcinogenicity studies with male Fisher 344 rats (Sakamoto *et al.*, 2009) and male C57BL/6-originated mice that were heterozygously deficient in the *p53* gene (Takagi *et al.*, 2008); these reports describe their physicochemical properties. Carbon black (CB; 22 nm in diameter) was purchased from Showa Chemical Industry Co., Ltd. (Tokyo, Japan). UICC-grade crocidolite was provided by the Tokyo Metropolitan Institute of Public Health.

Ovalbumin (OVA) and bovine serum albumin (BSA) were purchased from Sigma-Aldrich Co. (St. Louis, MO, USA). Horseradish peroxidase (HRP)-conjugated anti-mouse IgM and IgG_1 antibodies were purchased from Zymed Laboratories (South San Francisco, CA, USA). 2,2'-Azino-bis(3-ethylbenzothiazoline-6-sulfonic acid) diammonium salt (ABTS) tablets, a substrate for HPR-conjugated antibodies, were purchased from Roche Diagnostics Division (Basel, Switzerland). Monoclonal anti-OVA-IgG_1 antibody (clone OVA-14) was purchased from Sigma-Aldrich. Phycoerythrin-conjugated (PE-) anti-CD3 (derived from T cell clone 145-2C11), fluorescein isothiocyanate-conjugated (FITC-) anti-CD45R (B220) (derived from B cell clone RA3-6B2), PE- anti-CD8 (clone 53-6.7), and FITC- anti-CD4 (clone GK1.5) were purchased from Beckman Coulter, Inc. (Fullerton, CA, USA). PE-Cy5.5-anti-CD3 (clone 145-2C11), PE-Cy5.5-anti-CD45 (derived from leukocyte clone 30-F11), PE-anti-CD14 (derived from monocyte clone: Sa2-8), PE-anti-Ly-6G (derived from granulocyte clone RB6-8C5), FITC-anti-CD54 (intercellular adhesion molecule [ICAM]-1; clone YN1/1.7.4), FITC-anti-CD49d (integrin α4; clone R1-2), FITC-anti-CD11b (integrin αM; clone 1/70), and anti-CD16/CD32 (Fcγ receptor III/II; clone 93) antibodies were purchased from eBioscience, Inc. (San Diego, CA, USA). RNAprotect Cell Reagent, RNeasy Mini kit, High Capacity RNA-to-cDNA kit, TaqMan Gene Expression Master Mix, and TaqMan Gene Expression Assays Inventoried were purchased from Life Technologies Co. (Carlsbad, CA, USA).

Animal experiments

Three independent animal experiments were conducted; protocols for handling test chemicals were identical in each. MWCNTs, CB, or crocidolite was suspended in 2% sodium carboxymethyl cellulose (CMC Na) to a concentration of 0.2 mg/ml. A single intraperitoneal dose (2 mg/kg body weight) of each of these was administered to mice. In a vehicle control group, CMC Na was administered with a single intraperitoneal volume of 10 ml/kg body weight.

The first animal experiment included histopathological examination and real-time polymerase chain reaction (PCR) assays for mRNA expression of cytokine/chemokine genes. Within 32 weeks, 2 of 6 mice that were administered MWCNT died; hence, the last experiment was conducted at the end of 34 weeks after administration. Mice were maintained up to 34 weeks after their exposure to test chemicals or vehicle. From each treatment or vehicle group, 3-6 animals were chosen for assays at the end of 2, 4, 10, 20, and 34 weeks. Under light ether anesthesia, cells were collected from the abdominal cavity and suspended in 5 ml of phosphate-buffered saline (PBS), centrifuged at 1,200 rpm for 10 min, and stored in RNAprotect Cell Reagent until RNA extraction for the real-time PCR assay. Tissues and organs were harvested for histopathological examinations. Samples were fixed in neutrally buffered formalin, embedded in paraffin, and stained with sirius red for collagen or hematoxylin-eosin.

The second animal experiment included flow cytometry analysis of the peripheral blood cells. Mice were maintained up to 20 weeks after their exposure to test chemicals or vehicle. From each treatment or vehicle group, 4 animals were chosen for the assays on day 2 and at the end of 1, 2, 4, and 20 weeks. Under light ether anesthesia, approximately 1 ml of blood was collected through cardiac puncture into a syringe with 20 μl of an anticoagulant, ethylenediaminetetraacetic acid, and used for flow cytometry.

The third animal experiment included determinations of OVA-specific immunoglobulins. After their exposure to test chemicals or vehicle, mice were immunized with OVA/alum intraperitoneally administered at a dose of 100 μg/mouse on days 2 and 10 as previously described (Ito *et al.*, 2002). Under light ether anesthesia, blood samples of approximately 0.1 ml were collected from a tail vein. Samples were taken from 10 to19 animals from each treatment or vehicle group from the tail vein 8 days after the last immunization for IgM and from 15 animals from each group 20 days after the last immunization for IgG_1. Serum was stored at -80°C until assayed.

Real-time PCR assays for mRNA expression of cytokine/chemokine gene

Total RNA was isolated from 5 x 10^4 peritoneal cells obtained in the first animal experiment as described above, using RNeasy Mini kit. RNA from untreated 8-16-week-old female ICR mice were prepared separately, pooled, and used as a basal expression control. First-strand cDNA was prepared from 0.9 μg of RNA using a High Capacity RNA-to-cDNA kit. PCR used TaqMan Gene Expression Master Mix for genes (*IL-1β*, Mm01336189_m1; *IL-2*, Mm00434256_m1; *IL-4*, Mm99999154_m1; *IL-5*, Mm99999063_m1; *IL-6*, Mm99999064_m1; *IL-8*, Mm00436450_m1; *IL-10*, Mm99999062_m1; *IL-13*, Mm00434204_m1; *IL-17*, Mm00439619_m1; *IL-18*, Mm00434225_m1; *IL-33*, Mm00505403_m1; *IFNγ*, Mm99999071_m1; *MCP-1*, Mm00441242_m1; *MyD88*, Mm00440338_m1; *TGFβ1*, Mm03024053_m1; *TNFα*, Mm99999068_m1; *TATA box binding protein [TBP]*, Mm00446973_m1; *hypoxanthine phosphoribosyltransferase [HPRT]*, Mm00446968_m1), cDNA-specific TaqMan Gene Expression Assays, and an ABI 7500 Real-Time PCR System (Life Technologies). All PCR reactions were performed in duplicates. The quantity of PCR product was determined by the Comparative Ct Method as described by the manufacturer, in which each sample was normalized against the value of a housekeeping gene, *HPRT*. Fold-changes were expressed as either an increase or decrease compared with the basal expression control level.

Flow cytometry analysis of the peripheral blood cells

After 15 minute pre-incubation with an anti-CD16/32 monoclonal antibody to prevent non-specific binding, a peripheral blood sample (100 μl) obtained in the second animal experiment described above was reacted with various combinations of antibodies. After a 30-min incubation in the dark, erythrocytes were lysed with 4 ml of Tris (1 g/500 ml)plus NH_4Cl (2.8 g /500 ml) for 10 min, suspended in 4 ml of PBS, and centrifuged at 1,200 rpm for 10 min. The cell pellet was washed in PBS with 0.5% BSA. Fluorescence intensity and cell numbers were determined using a Cell Lab Quanta SC (Beckman Coulter). The number of leucocytes was counted as positive cells of PE-Cy5.5- anti-CD45 antibody. The number of lymphocytes was distinguished based on CD45 fluorescence and side scatter. T and B cells were distinguished based on PE and FITC fluorescence from PE-Cy5.5- CD45 positive cells. CD4 and CD8 cells were distinguished based on PE and FITC fluorescence from PE-Cy5.5- CD3 positive cells. Percent of CD11b, CD49d, and CD54 positive cells was measured based on FITC fluorescence from CD45 and CD14 or CD45 and Ly6G positive cells.

Serum OVA-specific immunoglobulin concentrations

Concentrations of OVA-specific IgM and IgG_1 in serum were determined using ELISA. We added 100 μl of 100 μg/ml of OVA to wells of a microtest plate and incubated the plates overnight at 4°C. Wells were washed 6 times with 0.05% Tween20/PBS (0.05T/PBS) and blocked with 5% BSA in PBS (5B/PBS) for 2 hr at room temperature. Diluted serum (IgM: 1/150, IgG_1: 1/5 x 10^6) was then added to each well and incubated for 2 hr. After 6 washes with 0.05T/PBS, the wells were blocked with 5B/PBS for 1 hr at room temperature. HRP-labeled anti-mouse IgM and IgG_1 antibodies were added to each well, and the plates were incubated for 2 hr at room temperature. After 6 washes with 0.05T/PBS, a substrate solution prepared using ABTS Tablets according to the manufacturer's instructions was added and the color reaction was allowed to develop in the dark at room temperature for 30 min. Optical density (OD) at 405 against 492 nm was determined using a microplate reader (SUNRISE REMOTE; Wako Pure Chemical Industries, Ltd., Osaka, Japan). Values for anti-OVA antibody were used as basal expression control.

Statistical analysis

Intergroup comparisons were made using Student's *t*-test. Significance level was set at p value < 0.05 .

RESULTS

General findings

During the course of the experiments, the body weights of mice increased within the same range after intraperitoneal administration of CMC Na, MWCNTs, CB, or crocidolite. In the first animal experiment, morphological assessments were conducted for mice that were given a single intraperitoneal administration of MWCNT, CB, or crocidolite. In the abdominal cavities of MWCNT-treated mice as compared with CMC Na-treated mice, liver edges had lost their sharpness, fibrous adhesions were seen on internal organs, and deposits were observed on the surfaces of the liver and diaphragm (Figs. 1a and 1b). In CB-treated mice, deposits were scattered in the abdominal cavity, especially on intestinal surfaces (Fig. 1c). No noteworthy changes were observed in the abdominal cavities of the CMC Na- or crocidolite-treated mice (Figs. 1a and 1d), or anywhere outside of the abdominal cavity in any of the groups.

Peritoneal cells obtained from MWCNT-treated mice contained small amounts of erythrocytes as compared with CMC Na-treated mice (Figs. 2a and 2b), whereas numerous erythrocytes were found for the crocidolite-treated mice (Fig. 2d). The peritoneal cells obtained from the CB-treated mice looked black, presumably because of the engulfment of the test chemical (Fig. 2c).

Fig. 3 showed the micrograms of liver, and Fig. 3a and 3b were the liver of CMC Na treated-mice that had thin layered mesothelium. Histopathological examinations revealed that the hepatic visceral peritoneum had fibrous thickening along with mesothelial cell hypertrophy in the MWCNT-treated mice (Figs. 3c and 3d). Inflammatory cells had infiltrated into this fibrously thickened visceral peritoneum. The majority of these infiltrating cells were macrophages containing MWCNTs, along with eosinophils, plasma cells, and immature myeloid cells (Fig. 3e) that occasionally formed a granulation (Fig. 3c). These changes were not observed in the CB- or crocidolite-treated mice.

No tumorigenic changes were observed either macroscopically or histopathologically in any of the mice treated with any of the test chemicals within the 34-week experimental period.

Expression of cytokine mRNA in peritoneal cells

mRNA expression levels of certain cytokine genes were substantially increased in the peritoneal cells obtained from MWCNT-treated mice, and these high levels were maintained up to the ends of 20 and 34 weeks. Th2 cytokine gene mRNA levels for *IL-4*, *IL-5*, and *IL-13*

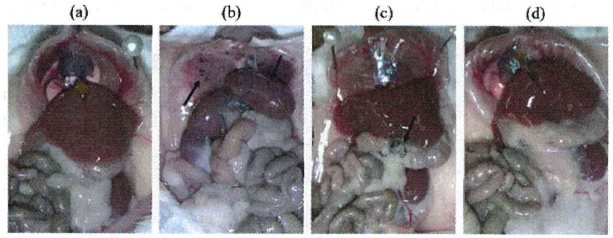

Fig. 1. Representative macroscopic appearances of the mouse abdominal cavity in the first animal experiment. Observations were made at 10 weeks after exposure to (a) CMC Na, (b) MWCNTs, (c) CB, or (d) crocidolite. Arrows indicate deposits of test chemicals.

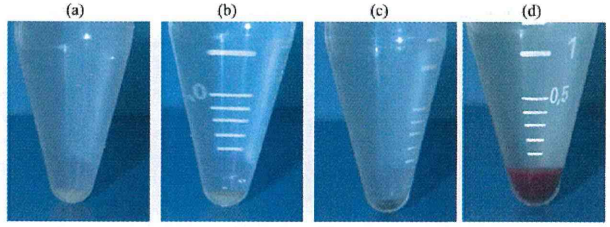

Fig. 2. Representative macroscopic appearances of peritoneal cells obtained from mice in the first animal experiment. Observations were made at 10 weeks after exposure to (a) CMC Na, (b) MWCNTs, (c) CB, or (d) crocidolite.

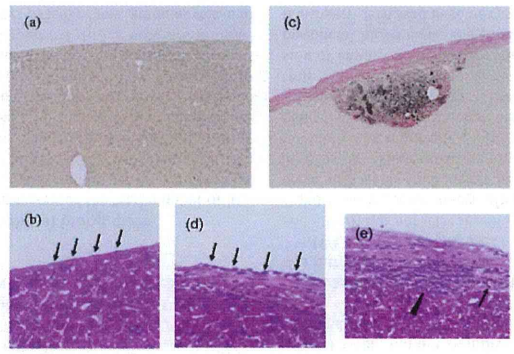

Fig. 3. Representative histology of the mouse liver in the first animal experiment. Examinations were made at 20 weeks after exposure to (a, b) CMC Na or (c-e) MWCNTs. Arrows indicate mesothelial cells and arrowheads indicate the infiltrations of eosinophils and immature myeloid cells. (a) and (c) were stained with sirius red staining, x 100, and (b), (d), and (e) were stained with hematoxylin-eosin, x 400.

were significantly increased from 2 to 20 weeks after administering MWCNTs. When compared with the basal expression control value for untreated animals, mRNA levels of *IL-4* were 34, 43, 24, 60, and 3 times higher, those of *IL-5* were 110, 127, 63, 226, and 69 times higher, and those of *IL-13* were 55, 38, 11, 28, and 3 times higher at 2, 4, 10, 20, and 34 weeks, respectively, after administering MWCNTs (Fig. 4).

Overexpression of mRNA of Th1 cytokine genes, *IL-2* and *IFNγ*, were delayed compared with mRNA of Th2 cytokine genes, but were also sustained; however, these were not significantly higher than basal expression levels except for *IL-2* at the end of 34 weeks. mRNA expression levels of *IL-2* were 0.3, 0.6, 1.5, 5.4, and 4.8 times higher, and those of *IFNγ* were 0.5, 0.3, 0.6, 1.6, and 4.3 times higher at the end of 2, 4, 10, 20, and 34 weeks, respectively (Fig. 4). Sustained mRNA overexpression was also found for a Th17 cytokine gene, *IL-17*, and these increases were significant at the end of 10 to 20 weeks.

mRNA for genes of proinflammatory cytokines, *IL-1β*, *IL-33*, and *TNFα*, and an inflammatory chemokine, *MCP-1*, were increased significantly at the end of 2 to 20 weeks (*IL-1β* and *TNFα*) and at 2 to 34 weeks (*IL-33* and *MCP-1*). mRNA level of an adapter protein of Toll-like receptors (TLR), *MyD88*, was also increased significantly at the end of week 2 to 20. mRNA levels of *IL-17* were 9, 13, 9, 26, and 25 times higher, those of *IL-1β* were 29, 23, 32, 28, and 19 times higher, those of *IL-33* were 13, 20, 5, 13, and 20 times higher, those of *TNFα* were 3, 2, 2, 3, and 2 times higher, those of *MCP-1* were 17, 28, 41, 49, and 42 times higher, and those of *MyD88* were 3, 3, 2, 2, and 1 time higher at 2, 4, 10, 20, and 34 weeks, respectively, after MWCNT administration (Figs. 4 and 5). mRNA levels of other inflammatory cytokine genes (*IL-6*, *IL-8,* and *IL-18*), anti-inflammatory cytokines (*IL-10* and *TGFβ*), and a housekeeping gene (*TBP*) were not affected by exposure to MWCNTs (Figs. 4 and 5).

CB did not affect these cytokine mRNA expressions in peritoneal cells. For crocidolite-treated mice, sustained mRNA overexpression was observed only for an inflammatory cytokine gene, *IL-6* (4, 5, 6, and 8 times higher at the end of 2, 4, 10, and 20 weeks, respectively), which

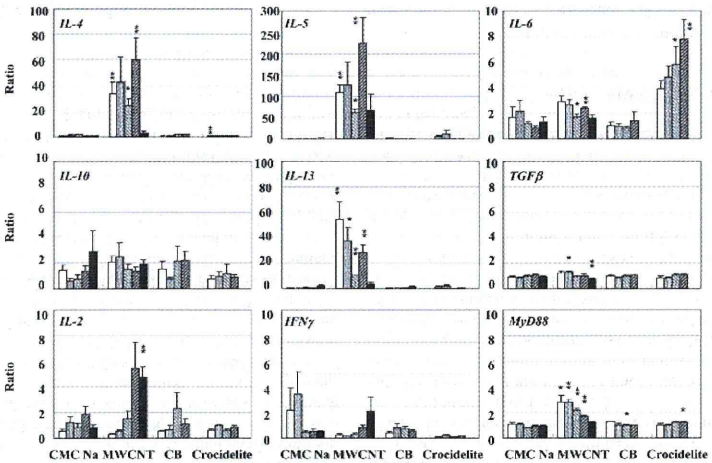

Fig. 4. mRNA expression of Th2 cytokine genes (*IL-4*, *IL-5*, *IL-10*, *IL-13*, and *TGFβ*), Th1 cytokine genes (*IL-2* and *IFNγ*), and a TLR adaptor protein (*MyD88*) in peritoneal cells obtained from mice in the first animal experiment. For each group of mice exposed to a test chemical or vehicle, columns from the left to the right are average values (n = 3-6) at 2, 4, 10, 20, and 34 weeks after exposure. These determinations were not made at the end of week 34 for the CB- and crocidolite-treated groups. (*$p < 0.05$, **$p < 0.01$).

was a more pronounced change than that with MWCNTs (Fig. 4). In addition, mRNA levels of *IL-5* were 5, 11, 1, and 1 times higher (Fig. 4), and those of *MCP-1* were 14, 9, 2, and 4 times higher (Fig. 5) at the end of 2, 4, 10, and 20 weeks, respectively; however, these changes were faint and transient.

Effects on the peripheral blood cells

MWCNT treatment increased the total number of leukocytes, granulocytes, and monocytes in the peripheral blood as early as 1 week after its administration, and these high levels were maintained up to the end of week 20 (Figs. 6a, 6b and 6c). The number of total lymphocytes was also increased, but only at the end of week 20. B and T cells were increased, although not significantly, within the 20-week experimental period in the MWCNT-treated mice (Figs. 6d, 6e and 6f). In the crocidolite treatment mice, the numbers of leukocytes, granulocytes, and monocytes exhibited a statistically significant, although minimal, transient increase at the end of week 1 (Figs. 6a, 6b and 6c). CB and crocidolite treatment increased the numbers of lymphocytes, B, and T cells at the end of day 2 and 1 week, but not significantly, and then decreased (Figs. 6d, 6e and 6f).

Expression of leukocyte adhesion molecules on the peripheral blood cells

MWCNT treatment induced overexpression of CD49d and CD54, but not CD11b, on granulocytes as early as 2 and 1 weeks, respectively, after its administration, and these high levels were maintained up to the end of week 20 (Fig. 7a). The expression of adhesion molecules was not altered on monocytes, with the exception that a statistically significant, although minimal, transient overexpression was observed for CD49d at the end of week 4 (Fig. 7b). CB and crocidolite did not induce overexpression of any of the leukocyte adhesion molecules on the peripheral blood cells, and in fact their expression was transiently decreased in some cases (Fig. 7).

OVA-specific immunoglobulins in serum

Figure 8 summarizes the results for the serum con-

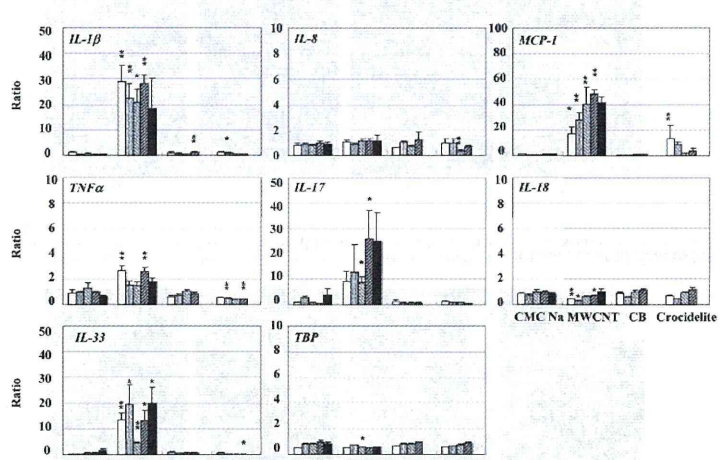

Fig. 5. mRNA expression of inflammatory cytokine genes in peritoneal cells obtained from mice in the first animal experiment. For each group of mice exposed to a test chemical or vehicle, columns from the left to the right are average values (n = 3-6) at 2, 4, 10, 20, and 34 weeks after exposure. These determinations were not made at the end of week 34 for the CB- and crocidolite-treated groups. (*$p < 0.05$, **$p < 0.01$).

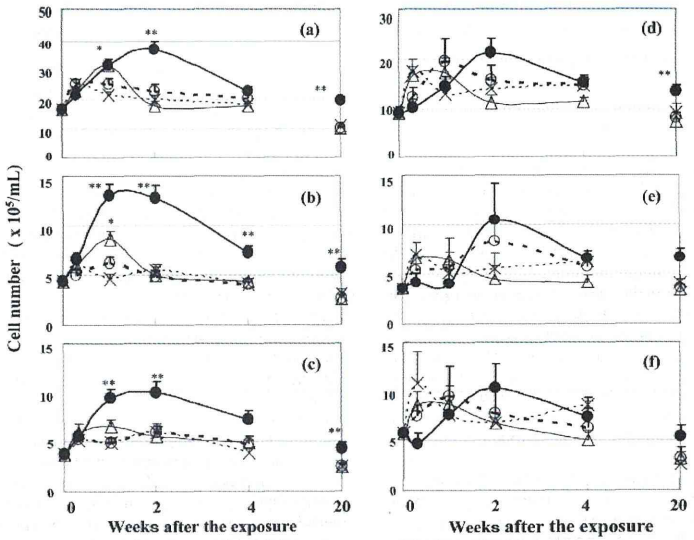

Fig. 6. Flow cytometry results for the peripheral blood cells obtained from mice in the second animal experiment. Changes in the numbers of (a) leukocytes, (b) granulocytes, (c) monocytes, (d) lymphocytes, (e) B cells, and (f) T cells after exposure to CMC Na (open circles), MWCNTs (closed circles), CB (crosses), and crocidolite (open triangles). Results are means ± standard deviations (n = 4). Asterisks indicate that results are significantly different from those of controls (*$p < 0.05$, **$p < 0.01$).

centrations of OVA-specific IgM (Fig. 8a) and IgG_1 (Fig. 8b). For mice treated with MWCNTs, CB, crocidolite, and CMC Na, the relative amounts (arbitrary units; AU) of OVA-specific IgM were, 1.33 ± 0.20, 1.07 ± 0.20, 1.07 ± 0.15, and 0.79 ± 0.12 AU, respectively, while those for OVA-specific IgG_1 were, 3.68 ± 0.57, 2.49 ± 0.29, 2.13 ± 0.32, and 2.28 ± 0.35 AU, respectively. Thus, MWCNT and not CB or crocidolite, significantly enhanced the production of OVA-specific immunoglobulins in mice.

DISCUSSION

The present study clearly shows that MWCNTs stimulated immune and inflammatory responses in mice and these effects sustained until the mice died. It has been previously shown in other animal models that a single intraperitoneal administration of MWCNT caused severe inflammation throughout the abdominal cavity and mesothelioma. Male Fisher 344 rats died at 37-52 weeks after administration (Sakamoto *et al.*, 2009) and and male C57BL/6-originated mice heterozygously deficient in the *p53* gene died within 25 weeks of administration (Takagi *et al.*, 2008).

The toxicity caused by MWCNTs in the present study did not involve tumor formation, but did induce severe inflammation, and 2 of 6 mice had died by the end of 32 weeks. The differences in the magnitudes of MWCNT toxicity between the present and previous studies was apparently because of differences in species, strains, and/or genders. To extrapolate the animal toxicity data to information important for human health concerns, further investigations are required. The most aggressive morphological change we observed was the infiltration of macrophages, eosinophils, plasma cells, and immature myeloid cells into the fibrously thickened visceral peritoneum of the liver with occasional granulation, and severe fibrous adhesions to the internal organs.

Light microscopic examination revealed that MWCNT

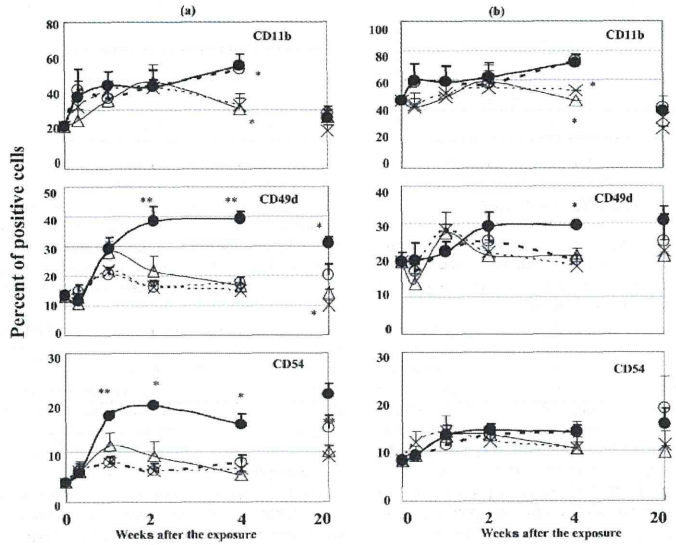

Fig. 7. Flow cytometry results for the peripheral blood cells obtained from mice in the second animal experiment. Changes in the expression of adhesion molecules on the surfaces of (a) granulocytes and (b) monocytes after exposure to CMC Na (open circles), MWCNT (closed circles), CB (crosses), and crocidolite (open triangles). Results are means ± S.D. (n = 4). Asterisks indicate that values are significantly different from those of controls (*$p < 0.05$).

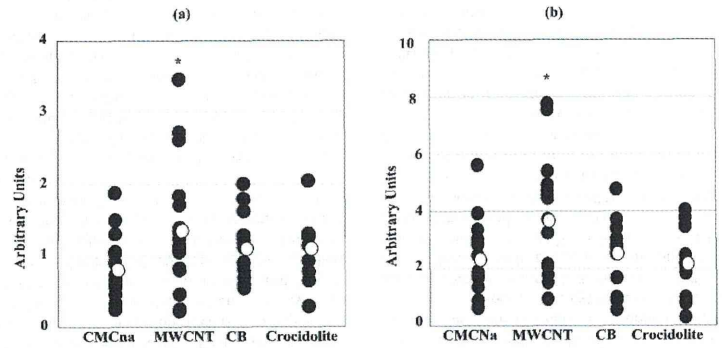

Fig. 8. Production of OVA-specific antibodies by mice in the third animal experiment. Serum concentrations of OVA-specific (a) IgM and (b) IgG_1 Open circles are average values, and closed circles are individual values (n = 10-19 for IgM, and n = 15 for IgG_1). Asterisks indicate that values are significantly different from those of controls (*$p < 0.05$).

were present in macrophages in these lesions. Frustrated phagocytosis has frequently been postulated to be involved in the mechanisms by which MWCNTs causes toxicity, including inflammation and carcinogenesis (Poland *et al.*, 2008). Thus, these lesions may have some fundamental biological importance. The sustained overexpression of cytokine mRNA in peritoneal cells may suggest one possibility, although no MWCNTs were observed in the peritoneal cells by light microscopy. An *in vitro* time lapse experiment revealed that dead cells with MWCNTs had been re-engulfed by other macrophages (data not shown), suggesting a cycle of sustained inflammation. MWCNTs either could not be limited by granuloma formation or subvisible MWCNTs may remain in the cavity. Thus, macrophages may continue their phagocytic activity, and as a result inflammatory cytokines/chemokines would be continuously produced.

Our results indicated that MWCNTs caused a systemic inflammation that was sustained for at least 20-34 weeks after a single intraperitoneal administration, because the numbers of leukocytes, granulocytes, and monocytes in the peripheral blood were increased from 1 to 20 weeks after MWCNT administration. During a similar period, CD49d and CD54 were overexpressed on granulocytes, which may have been involved in their infiltration into the inflammatory sites past vascular endothelial cells. Crocidolite increased the numbers of leukocytes, granulocytes, and monocytes at 1 week, but returned to the basal level after 2 weeks, and the effects were weaker than MWCNTs. The number of leukocytes was slightly increased at 2 days and 1 week after CMCNa exposure, and mRNA level of *IFNγ* was increased at 2 and 4 weeks after CMCNa exposure, but decreased thereafter. However the effect of CMCNa has not been known, there is a possibility CMCNa acts as a xenobiotic although the effect is little. Furthermore, the number of peripheral lymphocytes was also increased at 20 weeks after MWCNT administration, and this corresponded to the enhanced T cell-dependent production of OVA-specific antibodies, as indicated by their increased serum concentrations. The overexpressed mRNA of Th2 cytokine genes seen in peritoneal cells suggested that these cytokines have been involved in this enhanced antibody production. Although the underlying mechanisms need to be clarified, MWCNTs may promote these immune responses by acting as an adjuvant (Inoue *et al.*, 2009; Nygaard *et al.*, 2009).

The present study demonstrated the overexpression of mRNA for various cytokines/chemokines in peritoneal cells after a single intraperitoneal administration of MWCNTs. To the best of our knowledge, this is the first report of results obtained for peritoneal cells with regard to changes in cytokine/chemokine mRNA expression after MWCNT exposure *in vivo*. Previous reports focused primarily on short-term effects of MWCNT exposure. Mitchell *et al.* (2007) reported that *IL-10* levels increased in spleen homogenates after 14 consecutive days of whole body inhalation exposure for male C54BL/6 mice. Park *et al.* (2009) found that the protein levels of proinflammatory cytokines were increased both in the BAL fluid and in the peripheral blood, in which Th2 cytokines were increased to a greater extent than Th1 cytokines, in mice given intratracheal administrations of MWCNTs. In these reports, the levels of cytokines reached a peak at day 1 after the exposure and remained high at day 14.

In a study by Ryman-Rasmussen *et al.* (2009b) intratracheally administered MWCNTs potentiated the development of airway fibrosis in mice with allergic asthma induced by OVA sensitization, in which the levels of *IL-13* and *IL-5* increased at day 1, but returned to normal levels at day 14 when airway fibrosis became significant. Inoue *et al.* (2009) used MWCNT instillation for 6 weeks. At 24 hours after the final treatment, they observed significant exacerbation of murine allergic airway inflammation and high levels of Th1 and Th2 cytokine proteins. In the present study, the time-courses of changes in mRNA levels corresponded to functional groups of cytokines/chemokines.

mRNA overexpression of some pro-inflammatory cytokine genes, *IL-1β and IL-33*, occurred within 2 weeks and remained elevated up to the end of week 34. These are known to induce Th2 cytokines (Schmitz *et al.*, 2005; Amatucci *et al.*, 2007; Komai-Koma *et al.*, 2007; Kondo *et al.*, 2008). Therefore, mRNA of Th2 cytokine genes, *IL-4*, *IL-5* and *IL-13*, were also overexpressed within 2 weeks and remained elevated up to week 20. Among these, mRNA level for *IL-5* was still high, but levels for *IL-4* and *IL-13* decreased at the end of week 34.

mRNA level of a Th17 cytokine gene, *IL-17*, was also increased within 2 weeks, it was increased significantly after 10 to 20 weeks, and was still high, although not significantly, at the end of week 34. mRNA of Th1 cytokine genes, *IL-2* and *IFNγ*, were also overexpressed; however, this occurred at 20-34 weeks (*IL2*) and 34 weeks (*IFNγ*) after MWCNT exposure. While the details of the underlying mechanisms need to be clarified, the differential, time-dependent overexpression of Th2 and Th17 cytokine genes at first followed by Th1 cytokine genes may provide for some optimum balance between these inflammatory mediators for the sustained stimulating effects of MWCNTs on immune and inflammatory responses.

The present study indicated a rapid, drastic and sustained increase in mRNA levels of Th2 cytokine genes, *IL-4*, *IL-5*, and *IL-13*, in peritoneal cells after exposure to MWCNT. In asthmatic and atopic patients, Th2 cytokines are induced and enhance inflammation and fibrosis (Schmid-Grendelmeier *et al.*, 2002; Izuhara 2003; Doherty and Broide 2007; Choi *et al.*, 2008). Thus, the overexpression of the Th2 cytokine genes in the present study may indicate their critical roles in MWCNT-induced inflammatory changes.

Among these overexpressed Th2 cytokines, mRNA level of *IL-5* increased most strikingly; it was 100 times higher than the control level at the end of week 2 and 50 times higher even at the end of week 34. Administration of an anti-*IL-5* antibody to mild atopic asthmatic patients reduced the numbers of airway eosinophils and fibrosis (Flood-Page *et al.*, 2003), and that *IL-5* deficient mice have significantly less peribronchial fibrosis (total collagen content) and significantly less peribronchial smooth muscle (thickness of peribronchial smooth muscle layer, α-smooth muscle actin immunostaining; Cho *et al.*, 2004). Thus, *IL-5* may be biologically important in the inflammatory reactions related to immune system disturbances. In these reports, *IL-5* and *TGFβ* were involved in the infiltration of eosinophils. Although the mRNA level of *TGFβ* was not altered in the present study, *IL-5* overexpresion may have caused the eosinophil infiltration into inflammatory sites.

It has recently been shown that *IL-1β, IL-18*, and *IL-33* are produced by the innate immune system, followed by the subsequent induction of Th2 cytokines (Schmid-Grendelmeier *et al.*, 2002; Izuhara, 2003; Doherty and Broide, 2007; Choi, *et al.*, 2008; Kroeger, *et al.*, 2009). Microbial pathogens, dead cells, and foreign bodies, such as asbestos or silica, can impose stress on phagocytes, which then develop inflammasomes.

The inflammasome is a multi-protein complex that is activated by ligand-induced intermediates, such as reactive oxygen species (ROS), K^+ efflux, or by lysosome destabilization (Dostert *et al.*, 2008; Petrilli *et al.*, 2007; Hornung *et al.*, 2008), and then by cysteine protease caspase-1. (Martinon *et al.*, 2002). Caspase-1 can initiate an apoptotic pathway and, at the same time, cleave cytokine precursors, such as pro-*IL-1β* and pro-*IL-18*, to form their mature forms (Dostert *et al.*, 2008; Yazdi *et al.*, 2010).

IL-33 is another member of the *IL-1* family that is produced by endothelial cells, epithelial cells (Moussion *et al.*, 2008), and myeloid cells (Schmitz *et al.*, 2005; Nile *et al.*, 2010). *IL-33* is processed by caspases in a manner similar to *IL-1β* and *IL-18* during apoptosis, although its cleavage product is not biologically active, and the full active form of *IL-33* must be released from damaged or necrotic cells. *IL-1β, IL-18*, and *IL-33* have been shown to activate Th2 cells, eosinophils, basophils, and mast cells to produce Th2 cytokines (Chow *et al.*, 2010; Komai-Koma *et al.*, 2007; Kondo *et al.*, 2008; Schmitz *et al.*, 2005), which induce inflammatory, allergic, and fibrotic changes (Finkelman *et al.*, 1999; Choi *et al.*, 2008; Doherty and Broide 2007).

In the present study, the mRNAs of *IL-1β* and *IL-33*, but not *IL-18*, were shown to be overexpressed, which suggests the involvement of the innate immune system in MWCNT-induced inflammatory changes. This may also be supported by the observation of the mRNA overexpression of the TLR adapter protein gene *MyD88*. TLR-related signals can also activate caspase-1 and may be a minor pathway in MWCNT-induced innate immune responses, because the magnitude of the overexpression of *MyD88* was small, although significantly increased.

The present results indicate that MWCNTs exert stronger effects than CB or crocidolite in female ICR mice. The latter two did not cause any particular pathological changes, and there were no apparent increases in leukocyte numbers, increased expression of leukocyte adhesion molecules on the peripheral blood cells, or enhanced production of OVA-specific antibodies. In addition, CB did not induce overexpression of any cytokine mRNAs in peritoneal cells, even though phagocytic activity may have been involved for up to 20 weeks. In fact, previous reports described no adverse effects of CB (Tabet *et al.*,2009; Teeguarden *et al.*, 2011). Crocidolite caused a sustained overexpression of *IL-6* mRNA in peritoneal cells, but *IL-6* has been reported not to stimulate or injure vascular vessel permeability (Manhiani *et al.*, 2007; McClintock *et al.*, 2005).

In conclusion, under the present experimental conditions, MWCNTs exhibited sustained stimulating effects on immune and inflammatory responses, unlike the other mineral fibers with structural similarities.

ACKNOWLEDGMENTS

The authors thank Messrs. Katsuhito Yuzawa and Akimichi Nagasawa for their superb technical assistance. This work was supported in part by a research budget of the Tokyo Metropolitan Government, Japan, and a Grant-in-Aid from the Ministry of Health, Labour and Welfare of Japan.

REFERENCES

Amatucci, A., Novobrantseva, T., Gilbride, K., Brickelmaier, M., Hochman, P. and Ibraghimov, A. (2007): Recombinant ST2 boosts hepatic Th2 response in vivo. J. Leukoc. Biol., **82**, 124-132.

Cho, J.Y., Miller, M., Baek, K.J., Han, J.W., Nayar, J., Lee, S.Y., McElwain, K., McElwain, S., Friedman, S. and Broide, D.H. (2004): Inhibition of airway remodeling in IL-5-deficient mice. J. Clin. Invest., **113**, 551-560.

Choi, M., Cho, W.S., Han, B.S., Cho, M., Kim, S.Y., Yi, J.Y., Ahn, B., Kim, S.H. and Jeong, J. (2008): Transient pulmonary fibrogenic effect induced by intratracheal instillation of ultrafine amorphous silica in A/J mice. Toxicol. Lett., **182**, 97-101.

Chow, J.Y., Wong, C.K., Cheung, P.F. and Lam, C.W. (2010): Intracellular signaling mechanisms regulating the activation of human eosinophils by the novel Th2 cytokine IL-33: implications for allergic inflammation. Cell. Mol. Immunol., **7**, 26-34.

Doherty, T. and Broide, D. (2007): Cytokines and growth factors in airway remodeling in asthma. Curr. Opin. Immunol., **19**, 676-680.

Dostert, C., Petrilli, V., Van Bruggen, R., Steele, C., Mossman, B.T. and Tschopp, J. (2008): Innate immune activation through Nalp3 inflammasome sensing of asbestos and silica. Science, **320**, 674-677.

Finkelman, F.D., Wynn, T.A., Donaldson, D.D. and Urban, J.F. (1999): The role of IL-13 in helminth-induced inflammation and protective immunity against nematode infections. Curr. Opin. Immunol., **11**, 420-426.

Flood-Page, P., Menzies-Gow, A., Phipps, S., Ying, S., Wangoo, A., Ludwig, M.S., Barnes, N., Robinson, D. and Kay, A.B. (2003): Anti-IL-5 treatment reduces deposition of ECM proteins in the bronchial subepithelial basement membrane of mild atopic asthmatics. J. Clin. Invest., **112**, 1029-1036.

Hei, T.K., Piao, C.Q., He, Z.Y., Vannais, D. and Waldren, C.A. (1992): Chrysotile fiber is a strong mutagen in mammalian cells. Cancer Res., **52**, 6305-6309.

Hornung, V., Bauernfeind, F., Halle, A., Samstad, E.O., Kono, H., Rock, K.L., Fitzgerald, K.A. and Latz, E. (2008): Silica crystals and aluminum salts activate the NALP3 inflammasome through phagosomal destabilization. Nat. Immunol., **9**, 847-856.

Inoue, K., Koike, E., Yanagisawa, R., Hirano, S., Nishikawa, M. and Takano, H. (2009): Effects of multi-walled carbon nanotubes on a murine allergic airway inflammation model. Toxicol. Appl. Pharmacol., **237**, 306-316.

Ito, T., Inouye, K., Fujimaki, H., Tohyama, C. and Nohara, K. (2002): Mechanism of TCDD-induced suppression of antibody production: effect on T cell-derived cytokine production in the primary immune reaction of mice. Toxicol. Sci., **70**, 46-54.

Izuhara, K. (2003): The role of interleukin-4 and interleukin-13 in the non-immunologic aspects of asthma pathogenesis. Clin. Chem. Lab. Med., **41**, 860-864.

Komai-Koma, M., Xu, D., Li, Y., McKenzie, A.N., McInnes, I.B. and Liew, F.Y. (2007): IL-33 is a chemoattractant for human Th2 cells. Eur. J. Immunol., **37**, 2779-2786.

Kondo, Y., Yoshimoto, T., Yasuda, K., Futatsugi-Yumikura, S., Morimoto, M., Hayashi, N., Hoshino, T., Fujimoto, J. and Nakanishi, K. (2008): Administration of IL-33 induces airway hyperresponsiveness and goblet cell hyperplasia in the lungs in the absence of adaptive immune system. Int. Immunol., **20**, 791-800.

Kroeger, K.M., Sullivan, B.M. and Locksley, R.M. (2009): IL-18 and IL-33 elicit Th2 cytokines from basophils via a MyD88- and p38alpha-dependent pathway. J. Leukoc. Biol., **86**, 769-778.

Manhiani, M.M., Quigley, J.E., Socha, M.J., Motamed, K. and Imig, J.D. (2007): IL6 suppression provides renal protection independent of blood pressure in a murine model of salt-sensitive hypertension. Kidney Blood Press Res., **30**, 195-202.

Martinon, F., Burns, K. and Tschopp, J. (2002): The inflammasome: a molecular platform triggering activation of inflammatory caspases and processing of proIL-beta. Mol. Cell., **10**, 417-426.

McClintock, S.D., Barron, A.G., Olle, E.W., Deogracias, M.P., Warner, R.L., Opp, M and Johnson, K.J. (2005): Role of interleukin-6 in immune complex induced models of vascular injury. Inflammation, **29**, 154-162.

Mitchell, L.A., Gao, J., Wal, R.V., Gigliotti, A., Burchiel, S.W. and McDonald, J.D. (2007): Pulmonary and systemic immune response to inhaled multiwalled carbon nanotubes. Toxicol. Sci., **100**, 203-214.

Mossman, B.T., Bignon, J., Corn, M., Seaton, A. and Gee, J.B. (1990): Asbestos: scientific developments and implications for public policy. Science, **247**, 294-301.

Mossman, B.T. and Churg, A. (1998): Mechanisms in the pathogenesis of asbestosis and silicosis. Am. J. Respir. Crit. Care. Med., **157**, 1666-1680.

Moussion, C., Ortega, N. and Girard, J.P. (2008): The IL-1-like cytokine IL-33 is constitutively expressed in the nucleus of endothelial cells and epithelial cells in vivo: a novel 'alarmin'? PLoS One, **3**, e3331.

Nile, C.J., Barksby, E., Jitprasertwong, P., Preshaw, P.M. and Taylor, J.J. (2010): Expression and regulation of interleukin-33 in human monocytes. Immunology, **130**, 172-180.

Nygaard, U.C., Hansen, J.S., Samuelsen, M., Alberg, T., Marioara, C.D. and Lovik, M. (2009): Single-walled and multi-walled carbon nanotubes promote allergic immune responses in mice. Toxicol. Sci., **109**, 113-123.

Park, E.J., Cho, W.S., Jeong, J., Yi, J., Choi, K. and Park, K. (2009): Pro-inflammatory and potential allergic responses resulting from B cell activation in mice treated with multi-walled carbon nanotubes by intratracheal instillation. Toxicology, **259**, 113-121.

Petrilli, V., Papin, S., Dostert, C., Mayor, A., Martinon, F. and Tschopp, J. (2007): Activation of the NALP3 inflammasome is triggered by low intracellular potassium concentration. Cell Death Differ **14**, 1583-1589.

Poland, C.A., Duffin, R., Kinloch, I., Maynard, A., Wallace, W.A., Seaton, A., Stone, V., Brown, S., Macnee, W. and Donaldson, K. (2008): Carbon nanotubes introduced into the abdominal cavity of mice show asbestos-like pathogenicity in a pilot study. Nat. Nanotechnol., **3**, 423-428.

Porter, D.W., Hubbs, A.F., Mercer, R.R., Wu, N., Wolfarth, M.G., Sriram, K., Leonard, S., Battelli, L., Schwegler-Berry, D., Friend, S., Andrew, M., Chen, B.T., Tsuruoka, S., Endo, M. and Castranova, V. (2010): Mouse pulmonary dose- and time course-responses induced by exposure to multi-walled carbon nanotubes. Toxicology, **269**, 136-147.

Ryman-Rasmussen, J.P., Cesta, M.F., Brody, A.R., Shipley-Phillips, J.K., Everitt, J.I., Tewksbury, E.W., Moss, O.R., Wong, B.A., Dodd, D.E., Andersen, M.E. and Bonner, J.C. (2009a): Inhaled carbon nanotubes reach the subpleural tissue in mice. Nat. Nanotechnol., **4**, 747-751.

Ryman-Rasmussen, J.P., Tewksbury, E.W., Moss, O.R., Cesta, M.F., Wong, B.A. and Bonner, J.C. (2009b): Inhaled multiwalled carbon nanotubes potentiate airway fibrosis in murine allergic asthma. Am. J. Respir. Cell. Mol. Biol., **40**, 349-358.

Sakamoto, Y., Nakae, D., Fukumori, N., Tayama, K., Maekawa, A., Imai, K., Hirose, A., Nishimura, T., Ohashi, N. and Ogata, A. (2009): Induction of mesothelioma by a single intrascrotal administration of multi-wall carbon nanotube in intact male Fischer 344 rats. J. Toxicol. Sci., **34**, 65-76.

Schmid-Grendelmeier, P., Altznauer, F., Fischer, B., Bizer, C.,

Straumann, A., Menz, G., Blaser, K., Wüthrich, B. and Simon, H.U. (2002): Eosinophils express functional IL-13 in eosinophilic inflammatory diseases. J. Immunol., **169**, 1021-1027.

Schmitz, J., Owyang, A., Oldham, E., Song, Y., Murphy, E., McClanahan, T.K., Zurawski, G., Moshrefi, M., Qin, J., Li, X., Gorman, D.M., Bazan, J.F. and Kastelein, R.A. (2005): IL-33, an interleukin-1-like cytokine that signals via the IL-1 receptor-related protein ST2 and induces T helper type 2-associated cytokines. Immunity, **23**, 479-490.

Tabet, L., Bussy, C., Amara, N., Setyan, A., Grodet, A., Rossi, M.J., Pairon, J.C., Boczkowski, J. and Lanone, S. (2009): Adverse effects of industrial multiwalled carbon nanotubes on human pulmonary cells. J. Toxicol. Environ. Health A, **72**, 60-73.

Takagi, A., Hirose, A., Nishimura, T., Fukumori, N., Ogata, A., Ohashi, N., Kitajima, S. and Kanno, J. (2008): Induction of mesothelioma in p53+/- mouse by intraperitoneal application of multi-wall carbon nanotube. J. Toxicol. Sci., **33**, 105-116.

Teeguarden, J.G., Webb-Robertson, B.J., Waters, K.M., Murray, A.R., Kisin, E.R., Varnum, S.M., Jacobs, J.M., Pounds, J.G., Zanger, R.C. and Shvedova, A.A. (2011): Comparative proteomics and pulmonary toxicity of instilled single-walled carbon nanotubes, crocidolite asbestos, and ultrafine carbon black in mice. Toxicol. Sci., **120**, 123-135.

Yazdi, A.S., Guarda, G., Riteau, N., Drexler, S.K., Tardivel, A., Couillin, I. and Tschopp, J. (2010): Nanoparticles activate the NLR pyrin domain containing 3 (Nlrp3) inflammasome and cause pulmonary inflammation through release of IL-1alpha and IL-1beta. Proc. Natl. Acad. Sci. USA, **107**, 19449-19454.

Cancer Science
The official journal of the Japanese Cancer Association JCA

Multi-walled carbon nanotubes translocate into the pleural cavity and induce visceral mesothelial proliferation in rats

Jiegou Xu,[1,2] Mitsuru Futakuchi,[2] Hideo Shimizu,[3] David B. Alexander,[1] Kazuyoshi Yanagihara,[4] Katsumi Fukamachi,[2] Masumi Suzui,[2] Jun Kanno,[5] Akihiko Hirose,[6] Akio Ogata,[7] Yoshimitsu Sakamoto,[7] Dai Nakae,[7] Toyonori Omori[8] and Hiroyuki Tsuda[1,9]

[1]Laboratory of Nanotoxicology Project, Nagoya City University, Nagoya; [2]Department of Molecular Toxicology; [3]Core Laboratory, Nagoya City University Graduate School of Medical Sciences, Nagoya; [4]Department of Life Sciences, Yasuda Women's University Faculty of Pharmacy, Hiroshima; [5]Division of Cellular and Molecular Toxicology; [6]Division of Risk Assessment, National Institute of Health Sciences, Tokyo; [7]Department of Pharmaceutical and Environmental Sciences, Tokyo Metropolitan Institute of Public Health, Tokyo; [8]Department of Health Care Policy and Management, Nagoya City University Graduate School of Medical Sciences, Nagoya, Japan

(Received July 17, 2012/Revised August 20, 2012/Accepted August 22, 2012/Accepted manuscript online August 31, 2012/Article first published online October 10, 2012)

Multi-walled carbon nanotubes have a fibrous structure similar to asbestos and induce mesothelioma when injected into the peritoneal cavity. In the present study, we investigated whether carbon nanotubes administered into the lung through the trachea induce mesothelial lesions. Male F344 rats were treated with 0.5 mL of 500 μg/mL suspensions of multi-walled carbon nanotubes or crocidolite five times over a 9-day period by intrapulmonary spraying. Pleural cavity lavage fluid, lung and chest wall were then collected. Multi-walled carbon nanotubes and crocidolite were found mainly in alveolar macrophages and mediastinal lymph nodes. Importantly, the fibers were also found in the cell pellets of the pleural cavity lavage, mostly in macrophages. Both multi-walled carbon nanotube and crocidolite treatment induced hyperplastic proliferative lesions of the visceral mesothelium, with their proliferating cell nuclear antigen indices approximately 10-fold that of the vehicle control. The hyperplastic lesions were associated with inflammatory cell infiltration and inflammation-induced fibrotic lesions of the pleural tissues. The fibers were not found in the mesothelial proliferative lesions themselves. In the pleural cavity, abundant inflammatory cell infiltration, mainly composed of macrophages, was observed. Conditioned cell culture media of macrophages treated with multi-walled carbon nanotubes and crocidolite and the supernatants of pleural cavity lavage fluid from the dosed rats increased mesothelial cell proliferation *in vitro*, suggesting that mesothelial proliferative lesions were induced by inflammatory events in the lung and pleural cavity and likely mediated by macrophages. In conclusion, intrapulmonary administration of multi-walled carbon nanotubes, like asbestos, induced mesothelial proliferation potentially associated with mesothelioma development. (*Cancer Sci* 2012; 103: 2045–2050)

Multi-walled carbon nanotubes (MWCNT) are structurally composed of cylinders rolled up from several layers of graphite sheets. They are several to tens of nanometers in diameter and several to tens of micrometers in length. This high length to diameter aspect ratio, a characteristic shared with asbestos fibers, has led to concern that exposure to MWCNT might cause asbestos-like lung diseases, such as lung fibrosis, lung cancer, pleural plaque and malignant mesothelioma.[1–6]

Pleural plaque and malignant mesothelioma are characteristic lesions in asbestos-exposed humans. Although fiber dimensions, biopersistence, oxidative stress and inflammation have all been implicated,[7–12] the exact mechanisms of pleural pathogenesis are unclear. According to a pathogenesis paradigm suggested by Donaldson *et al.*,[2] asbestos fibers penetrate into the pleural cavity from the alveoli and deposit in the pleural tissue. Unlike spherical particles, fibrous materials such as asbestos are not cleared effectively from the pleural cavity, resulting in deposition of the fibers in the parietal pleura. This deposition, in turn, causes frustrated phagocytosis-induced pro-inflammatory, genotoxic and mitogenic responses in the deposition sites.[2]

Administration of MWCNT into the peritoneal cavity or scrotum in animals has been reported to induce mesothelial lesions, similar to those observed in asbestos cases.[13–15] The induction of mesothelioma in the peritonum is dose dependent, and is observed with as low as 3 μg/mouse in p53 heterozygous mice.[16] These studies suggest a potential risk that inhaled MWCNT might lead to pleural mesothelioma. However, actual experimental evidence demonstrating induction of pleural mesothelioma by inhaled MWCNT fibers has not yet been shown. It has been shown that inhaled MWCNT induced subpleural fibrosis with macrophage aggregates on the surface of the visceral pleura.[17] Notably, some of these macrophages contained MWCNT fibers. In addition, penetration of MWCNT administrated by pharyngeal aspiration into the pleural cavity was observed,[18] and intrapleural injection of 5 μg/mouse of MWCNT has been shown to lead to sustained inflammation and length-dependent retention of MWCNT in the pleural cavity.[19] Accordingly, direct interaction of MWCNT with the mesothelial tissue is postulated as an early pathogenic event.

In the present study, to examine whether MWCNT translocate into the pleural cavity and cause inflammation leading to proliferative change of the mesothelial tissue, we administered relatively high doses (five doses at 250 μg/rat) of two MWCNT samples (MWCNT-N and MWCNT-M) to the rat lung by intrapulmonary spraying (IPS)/intratracheal instillation; crocidolite (CRO; one kind of asbestos fiber) was used as a positive control. Intrapulmonary spraying has been shown to be an efficient method to deliver particle materials deep into the lung.[20–24] Our results demonstrated that MWCNT, like asbestos, translocated from the lung into the pleural cavity and induced inflammatory responses in the pleural cavity and, importantly, hyperplastic visceral mesothelial proliferation. These findings are important in understanding whether MWCNT have the potential to cause asbestos-like pleural lesions.

*To whom correspondence should be addressed.
E-mail: htsuda@phar.nagoya-cu.ac.jp

doi: 10.1111/cas.12005

Materials and Methods

Animals. Eight-week-old male F344 rats were purchased from Charles River Japan Inc. (Kanagawa, Japan). The animals were housed in the Animal Center of Nagoya City University Medical School and maintained on a 12 h light/12 h dark cycle, and received Oriental MF basal diet (Oriental Yeast Co. Ltd, Tokyo, Japan) and water *ad libitum*. The study was conducted according to the Guidelines for the Care and Use of Laboratory Animals of Nagoya City University Medical School and the experimental protocol was approved by the Institutional Animal Care and Use Committee (H22M-19).

Preparation of MWCNT and CRO suspensions. The MWCNT investigated were MWCNT-N (Nikkiso Co., Ltd, Tokyo, Japan) and MWCNT-7 (Mitsui Chemicals Inc., Tokyo, Japan; designated as MWCNT-M). Crocidolite (Union for International Cancer Control grade) was from the National Institute of Health Sciences of Japan stocks. Ten milligrams of MWCNT-N or MWCNT-M were suspended in 20 mL of saline containing 0.1% Tween 20 and homogenized for 1 min four times at 3000 r.p.m. in a Polytron PT1600E benchtop homogenizer (Kinematika AG, Littau, Switzerland). The suspensions were sonicated for 30 min shortly before use to minimize aggregation. The CRO suspension was prepared similarly, but without homogenization. The concentration of the MWCNT and CRO suspensions was 500 μg/mL. The lengths of MWCNT and CRO in the suspensions were determined using a digital map meter (Comcureve-9 Junior; Koizumi Sokki MFG. Co., Ltd, Nigata, Japan) on scanning electron microscope (SEM) photos. The SEM observation and length distributions of MWCNT and CRO are shown in Fig. S1A,B. To count the fiber number, 500 μg/mL suspensions of MWCNT-N, MWCNT-M and CRO were diluted 1:1000 with deionized water and 0.5 μL of the diluted suspensions was loaded onto clean glass slides and dried in a micro oven at 480°C for 1 min. The fiber number on the slides was counted under a polarized light microscope (PLM) (Olympus BX51N-31P-O PLM, Tokyo, Japan) (PLM detects all fibers longer than 200 nm). The results are shown in Fig. S1C.

Intrapulmonary spraying of MWCNT and CRO into the lung and pleural cavity lavage (PCL). We used the intrapulmonary spraying technique that was developed in our laboratory.[24] Briefly, rats were anaesthetized using isoflurane; the mouth was fully opened with the tongue gently held and the nozzle of a microsprayer (series IA-1B Intratracheal Aerosolizer; Penn-century, Philadelphia, PA, USA) was inserted into the trachea through the larynx and 0.5 mL suspension was sprayed into the lungs synchronizing with spontaneous respiratory inhalation. We confirmed that the dosed materials were distributed deep into the lung tissue and reached most of the terminal alveoli without causing obvious respiratory distress.

Ten-week-old male Fisher 344 rats were divided into four groups of six animals each and given 0.5 mL of saline containing 0.1% Tween 20 or 500 μg/mL MWCNT-N, MWCNT-M or CRO suspension by IPS once every other day five times over a 9-day period. The total amount of fibers administered was 1.25 mg/rat. Six hours after the last IPS, the rats were placed under deep isoflurane anesthesia; a small incision was made in the abdominal wall, the pleural cavity was injected with 10 mL of ice cold RPMI 1640 through the diaphragm, and the lavage fluid was collected by syringe. The rats were then killed by exsanguination from the inferior vena cava and the major organs, including the lung, chest wall, brain, liver, kidney, spleen and mediastinal lymph nodes, were fixed in 4% paraformaldehyde and processed for histological examination.

Analysis of inflammatory reaction in the pleural cavity. Cells in the lavage fluid were counted using a hemocytometer (Erma Co., Ltd, Tokyo, Japan), and the cellular fraction was then isolated by centrifugation at 200*g* for 5 min at 4°C. Cell pellets collected from three rats were combined (generating a total of two cell pellets per group), fixed in 4% paraformaldehyde and processed for histological examination. Total protein in the supernatants of each of the lavage fluids was determined using the Pierce BCA Protein Assay Kit (Thermo Scientific, Rockford, IL, USA) and the supernatants were then concentrated by centrifugation in Vivaspin 15 concentrators (Sartorius Stedium Biotech, Goettingen, Germany) at 1500*g* for 30 min at 4°C and used for *in vitro* cell proliferation assays.

Light microscopy and PLM. Haematoxylin–eosin (H&E)-stained slides of the lung tissues and cellular pellets of the PCL were used to observe MWCNT-N, MWCNT-M and CRO fibers with PLM at ×1000 magnification. The exact localization of the illuminated fibers was confirmed in the same H&E-stained sections after removing the polarizing filter.

Scanning electron microscopy. The H&E-stained slides of the lung tissue and PCL pellets were immersed in xylene for 3 days to remove the cover glass, then immersed in 100% ethanol for 10 min to remove the xylene and air-dried for 2 h at room temperature. The slides were then coated with platinum for viewing using a scanning electronic microscope (SEM) (Model S-4700 Field Emission SEM; Hitachi High Technologies Corporation, Tokyo, Japan) at 5–10 kV.

Immunohistochemistry and Azan–Mallory staining. CD68, proliferating cell nuclear antigen (PCNA) and mesothelin/Erc were detected using antirat CD68 antibodies (BMA Biomedicals, Augst, Switzerland), anti-PCNA monoclonal antibodies (Clone PC10; Dako Japan Inc., Tokyo, Japan) and antirat C-ERC/mesothelin polyclonal antibodies (Immuno-Biological Laboratories Co., Ltd, Gunma, Japan). The CD68, PCNA and C-ERC/mesothelin antibodies were diluted 1:100, 1:200 and 1:1000, respectively, in blocking solution and applied to deparaffinized slides. The slides were incubated at 4°C overnight and then incubated for 1 h with biotinylated species-specific secondary antibodies diluted 1:500 (Vector Laboratories, Burlingame, CA, USA) and visualized using avidin-conjugated horseradish peroxidase complex (ABC kit; Vector Laboratories). Azan–Mallory staining was used to visualize collagen fibers.

***In vitro* exposure and preparation of conditioned macrophage culture media.** The induction and preparation of primary alveolar macrophages (PAM) has been described previously.[24] PAM were seeded into 6 cm culture dishes at 2×10^6 cells per well in 10% FBS RPMI 1640. After overnight incubation, the culture media was refreshed and MWCNT-N, MWCNT-M or CRO suspensions were added to the cells to a final concentration of 10 μg/mL. The cells were then incubated for another 24 h. The conditioned macrophage culture media was then collected for *in vitro* cell proliferation assays.

***In vitro* cell proliferation assay.** Human mesothelioma cells, TCC-MESO1, derived from a patient in the Tochigi Cancer Center,[25] were seeded into 96-well culture plates at 2×10^3 cells per well in 10% FBS RPMI 1640. After overnight incubation, the cells were serum-starved for 24 h. The media was changed to 100 μL of the concentrated supernatants of the PCL or conditioned macrophage culture media and incubated for 72 h. The relative cell number was then determined using the Cell Counting Kit-8 (Dojindo Molecular Technologies, Rockville, MD, USA) according to the manufacturer's instruction.

Statistical analysis. Statistical analysis was performed using ANOVA. The statistical significance was analyzed using a two-tailed Student's *t*-test. A *P*-value of <0.05 was considered to be significant.

Results

Translocation of MWCNT and CRO fibers into the pleural cavity. The cell pellets of the PCL were used to examine whether

doi: 10.1111/cas.12005

the MWCNT or CRO fibers were present in the pleural cavity. We first screened the H&E-stained PCL cell pellet slides using PLM. The exact localization of the fibers was confirmed using SEM of the same slide sections. MWCNT-N, MWCNT-M and CRO fibers were present in PCL cell pellets, with most of the fibers in macrophage-like cells (Fig. 1a–c) with very few fibers located in the intercellular space or on cell surfaces (data not shown). Immunohistochemistry with CD68, a macrophage marker, showed that MWCNT and CRO fibers were mainly found in macrophages (Fig. 1d,e).

In tissue sections, MWCNT and CRO fibers were mainly detected in focal granulomatous lesions in the alveoli and in alveolar macrophages. Fibers were also found in the mediastinal lymph nodes, and a few fibers were detected in liver sinusoid cells, blood vessel wall cells in the brain, renal tubular cells and spleen sinus and macrophages (data not shown). We detected only a few fibers penetrating directly from the lung to the pleural cavity through the visceral pleura (Fig. S2) and did not find any fibers in the parietal pleura.

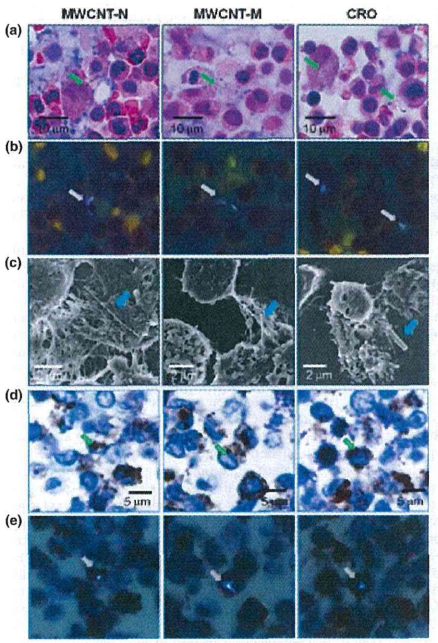

Fig. 1. Existence of multi-walled carbon nanotubes (MWCNT)-N, MWCNT-M and crocidolite (CRO) fibers in the cell pellets of the pleural cavity lavage (PCL). (a) Images of H&E-stained slides of the cell pellets of the PCL treated with MWCNT-N, MWCNT-M and CRO fibers. (b) Polarized light microscope (PLM) images of the same view areas shown in (a). (c) Scanning electron microscope observation showed the existence of the MWCNT and CRO fibers in the cell pellets of the PCL. (d) CD68 immunostaining of the PCL cell pellet slides. (e) PLM observation of the same view areas shown in (d) indicate that MWCNT and CRO fibers were present in the CD68-positive macrophages. Arrows indicate MWCNT-N, MWCNT-M and CRO fibers.

Induction of visceral mesothelial proliferation. Hyperplastic visceral mesothelial proliferation (HVMP) was clearly observed in all of the MWCNT and CRO treated groups. The HVMP lesions were composed of mesothelial cells with cuboidal appearance and increased size and density lining the visceral pleural tissue. Various degrees of lung inflammation and fibrous thickening were observed underneath the HVMP lesions (Fig. 2a, panel A). The PCNA immunostaining showed proliferating mesothelial cells within the HVMP lesions (Fig. 2a, panel B). The PCNA indices of the visceral mesothelium were increased approximately 10-fold in all the MWCNT and CRO treated groups compared with the control group

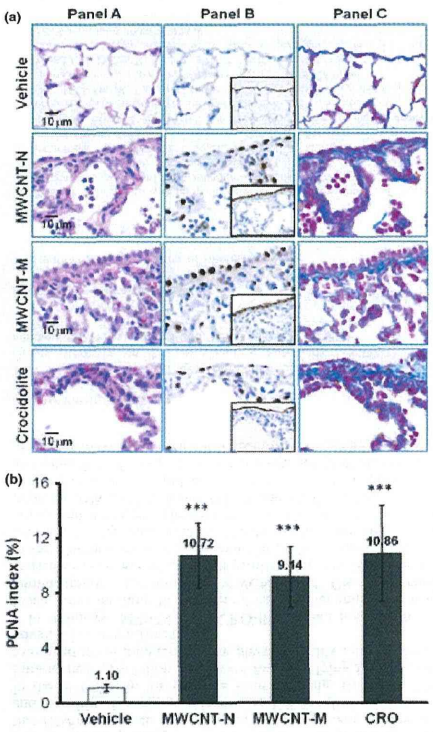

Fig. 2. Induction of visceral mesothelial cell proliferation lesions by treatment with multi-walled carbon nanotubes (MWCNT)-N, MWCNT-M or crocidolite (CRO). (a) Serial sections were prepared and stained with H&E, proliferating cell nuclear antigen (PCNA), Erc/mesothelin and Azan–Mallory's collagen staining. Panel A: increase in enlarged visceral mesothelial cells with cuboidal shapes in the MWCNT-N, MWCNT-M and CRO treated groups. Panel B: PCNA-positive cells are clearly increased in the dosed groups. The inserts are immunostained with Erc/mesothelin and show the lining of the mesothelium. Panel C: Azan–Mallory's staining; sub-pleural collagenous fibrosis is present under the mesothelial cell proliferation lesions. (b) PCNA index, expressed as the percentage of PCNA-positive cells of the total number of visceral mesothelial cells per slide. ***$P < 0.001$.

(Fig. 2b). Azan–Mallory staining showed increases in collagen fibers underneath the HVMP lesions (Fig. 2a, panel C). Fibers were not found within the HVMP lesions themselves. Alveolar macrophages with phagocytosed MWCNT or CRO fibers were frequently observed near the HVMP lesions (Fig. S3). Proliferation and other lesions of the parietal mesothelium were not observed.

Inflammatory cell infiltration in the pleural cavity. Both MWCNT and CRO treatment resulted in inflammatory reactions in the pleural cavity. The total number of cells, composed mostly of macrophages, neutrophils and lymphocytes, in the PCL in the MWCNT and CRO treated groups was significantly increased compared with the control group (Fig. 3a). As can be calculated from Fig. 3(a,b), macrophages accounted for a large part of the increase of the total cell number in the PCL, although the number of neutrophils and lymphocytes also increased. Overall, the proportion of macrophages in the cell pellets of the PCL was increased, while those of neutrophils and lymphocytes were decreased (Fig. 3b). MWCNT or CRO treatment also significantly increased the total protein level in the PLC (Fig. 3c). The proportion of cells in the PCL pellets

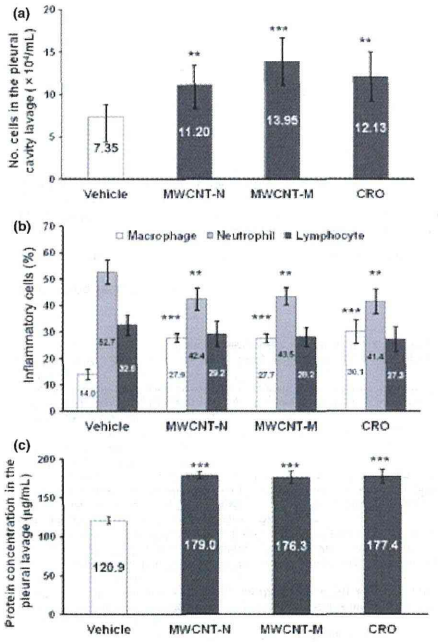

Fig. 3. Inflammatory reaction in the pleural cavity. (a) The number of leukocytes in the pleural cavity lavage (PCL) of rats treated with multi-walled carbon nanotubes (MWCNT) and crocidolite (CRO). (b) The proportion of macrophages, neutrophils and lymphocytes in the cell pellets of the PCL. Total cell number and cell numbers of macrophages, neutrophils and lymphocytes in 10 randomly chosen fields (×400) were counted. (c) Protein concentration in the supernatants of the PCL. **$P < 0.01$; ***$P < 0.001$.

positive for Mesothelin/Erc, a mesothelial cell marker, was 0.53–1.02%, and no intergroup difference was observed (data not shown). These data indicate that the increased cell number in the pleural cavity of the rats treated with MWCNT or CRO resulted from inflammatory cell effusion, not from mesothelial cell shedding of the pleural tissue. Many macrophages in the PCL contained MWCNT or CRO fibers.

Mesothelial cell proliferation assay *in vitro*. To examine whether inflammatory reactions, especially those mediated by macrophages, exert proliferative effects on mesothelial cells, we examined the effects of conditioned macrophage culture medium on mesothelial cell proliferation *in vitro*. The conditioned culture media of macrophages exposed to MWCNT-N, MWCNT-M or CRO significantly increased the proliferation of the human mesothelioma cell line TCC-MESO1. The concentrated supernatants of the PCL taken from the rats treated with MWCNT-N, MWCNT-M or CRO exhibited similar effects (Fig. 4). These results indicate that factors in the PCL, possibly secreted by alveolar and pleural macrophages, are able to cause mesothelial cell proliferation.

Discussion

In the present study, we compared the pleural translocation of MWCNT and CRO and examined the mesothelial lesions they induced. Our data demonstrate that after deposition in the lung, MWCNT, like CRO, translocated into the pleural cavity, mainly in pleural macrophages. Both MWCNT and CRO treatment also caused hyperplastic visceral mesothelial proliferation and marked pleural inflammation.

This is the first report to show that MWCNT administered into the rat lung causes mesothelial proliferative lesions. Adamson *et al.*[26] reported that intratracheal instillation of asbestos in mice induced pleural mesothelial cell proliferation within several days; the degree of pleural mesothelial cell proliferation did not appear to correlate with the localization of asbestos fibers in the pleura.[27] Similarly, we did not find fibers within the HVMP lesions. Thus, our findings suggest that HVMP lesions do not appear to be directly induced by the deposited MWCNT or CRO fibers. Also, *in vitro* exposure to MWCNT and CRO fibers did not lead to proliferation of TCC-MESO1 cells, but rather to cell death (Fig. S4). It has been reported that macrophages play a significant role in mesothelial cell proliferation caused by asbestos exposure and surgical injury,[28–31] and that the conditioned medium of macrophages

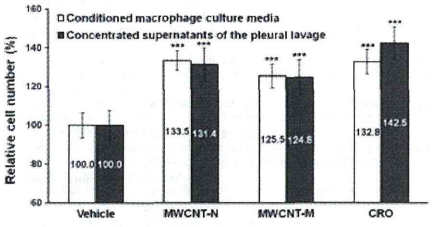

Fig. 4. Effect of conditioned macrophage culture media and the supernatants of the pleural cavity lavage (PCL) on mesothelial cell proliferation *in vitro*. The conditioned culture media of macrophages treated with multi-walled carbon nanotubes (MWCNT)-N, MWCNT-M or crocidolite (CRO) significantly increased the cell proliferation of TCC-MESO1. The concentrated supernatants of the PCL from the rats treated with MWCNT-N, MWCNT-M or CRO had similar effects. $n = 6$. ***$P < 0.001$.

doi: 10.1111/cas.12005